UNIVERSITY OF CALIFORNIA

Santa Barbara

Environmental Drivers of Giant Kelp Biomass and Physiological Condition

through Space and Time

A dissertation submitted in partial satisfaction of the

requirements for the degree Doctor of Philosophy

in Marine Science

by

Thomas William Bell III

Committee in charge:

Professor David Siegel, Chair

Professor Mark Brzezinski

Dr. Norman Nelson

Dr. Daniel Reed

Professor Dar Roberts

September 2016

The dissertation of Thomas William Bell III is approved.

_____

Mark Brzezinski

_____

Norman Nelson

_____

Daniel Reed

_____

Dar Roberts

_____

David Siegel, Committee Chair

September 2016

Environmental Drivers of Giant Kelp Biomass and Physiological Condition

through Space and Time

ACKNOWLEDGEMENTS

Finally, I wanted to acknowledge my friend, collaborator, and life partner Dana Morton for all the help, advice, and support she has given me throughout the years. Dana was studying the ocean years before I decided try it and has served as a sounding board for theories, methods, and ideas since at least the summer of 2009. Dana has been a source of inspiration and can't wait to see what she will do. This dissertation is dedicated to her.

VITA OF THOMAS WILLIAM BELL III
September 2016

Education

B.A. Integrative Biology, B.A. Legal Studies, University of California, Berkeley, December 2006
M.Sc. Biology (Ecology), San Diego State University, December 2011
Ph.D. in Marine Science, University of California, Santa Barbara, September 2016

Honors and Awards

UC Affiliates Graduate Dissertation Fellowship 2015
Brython Davis Endowment Graduate Fellowship 2015
NASA Earth and Space Science Fellowship 2012

Publications

Cabral, R.B., Gaines, S.D., Johnson, B., Bell. T.W., White, C. *in press*. Drivers of redistribution of fishing and non-fishing effort after the implementation of a marine protected area network. *Ecological Applications*.

Biederman, J.A., Scott, R.L, Goulden, M.L., Vargas, R., Litvak, M.E., Kolb, T.E., Yepez, E.A., Oechel, W.C., Blanken, P.D., Bell, T.W., Garatuza-Payan, J., Maurer, G.E., Dore, S., Burns, S.P. (2016) Contrasting effects of fast interannual and slow climatic precipitation variability on ecosystem carbon balance. *Global Change Biology,* 22, 1867-1879.

Young, M.A., Cavanaugh, K.C., Bell, T.W., Raimondi, P.T., Edwards, C., Drake, P., Erikson, L., Storlazzi, C. (2016) Explaining and predicting spatial patterns of persistence of giant kelp, *Macrocystis pyrifera*, forests in central California. *Ecological Monographs,* 86(1), 45-60.

Morton, D.N., Bell, T.W., Anderson, T.W. (2016) Spatial synchrony of amphipods in giant kelp forests. *Marine Biology,* 163(2), 1-11.

Castorani, M.C.N., Reed, D.C., Alberto, F., Bell, T.W., Simons, R. Cavanaugh, K.C., Siegel, D.A., Raimondi, P.T. (2015) Connectivity predicts local extinction and colonization in a marine metapopulation. *Ecology*, 96, 3142-3152.

Bell, T.W., Cavanaugh, K.C., Reed, D.C., Siegel, D.A. (2015) Geographical variability in the controls of giant kelp biomass dynamics. *Journal of Biogeography*, 42, 2010-2021.

Johansson, M.L., Alberto, F., Reed, D.C., Raimondi, P.T., Coelho, N.C., Young, M.A., Drake, P.T., Edwards, C.A., Cavanaugh, K.C., Assis, J., Ladah, L.B., Bell, T.W., Coyer, J.A., Siegel, D.A., Serrão, E.A. (2015) Seascape drivers of *Macrocystis pyrifera* population genetic structure in the eastern North Pacific. *Molecular Ecology*, 24, 4866-4885.

Bell, T.W., Cavanaugh, K.C., Siegel, D.A. (2015) Remote monitoring of giant kelp biomass and photosynthetic condition: An evaluation of the potential for the Hyperspectral Infrared Imager (HyspIRI) mission. *Remote Sensing of Environment*, 167, 218-228.

Bell, T.W., Menzer, O., Troyo-Diéquez, T., Oechel, W. (2012) Variation of Carbon Exchange over Multiple Temporal Scales in an Arid Shrub Ecosystem near La Paz, Baja California Sur, Mexico. *Global Change Biology*, 18, 2570-2582.

Professional Experience

Teaching Associate (*Instructor of Record*) – Biogeography: The Study of Plant and Animal Distributions (Geography 167), UCSB, Santa Barbara, CA, June – July 2016
Teaching Associate (*Instructor of Record*) – Marine Resources of the CA Current (Geography 158), UCSB, Santa Barbara, CA, September – December 2015
Teaching Associate (*Instructor of Record*) – Intermediate Remote Sensing Techniques (Geography 115C), UCSB, Santa Barbara, CA, April – June 2015

Selected Professional Presentations:

Assessment of Giant Kelp Physiological State Using Airborne Hyperspectral Imagery, Ocean Sciences Meeting, New Orleans, LA, February 2016
Long-term Monitoring of Giant Kelp Biomass Dynamics Exposes Nonlinear Relationships with Environmental Drivers, Western Society of Naturalists, Sacramento, CA, November 2015
Potential of the HyspIRI mission for monitoring the physiological condition of giant kelp forests, HyspIRI Science Workshop, Cal Tech, Pasadena, CA, October 2015
Temporal and spatial variability in the photosynthetic condition of giant kelp, Western Society of Naturalists, Tacoma, WA, November 2014
Primary drivers of giant kelp biomass in California, Western Society of Naturalists, Oxnard, CA, November 2013
Variation of Carbon Exchange over Multiple Temporal Scales in an Arid Shrub Ecosystem near La Paz, Mexico, Oxford Interdisciplinary Desert Conference, Oxford, England, March 2012
Vertical and Lateral Carbon Flux in Leaf Litter in a Larrea/Cardon Ecosystem near La Paz, Mexico, European Geosciences Union, Vienna, Austria, April 2011

ABSTRACT

Environmental Drivers of Giant Kelp Biomass and Physiological Condition

through Space and Time

by

Thomas William Bell III

The giant kelp (*Macrocystis pyrifera*) is a globally distributed foundation species, which supports an incredibly productive ecosystem. While this species has been well studied over the past several decades, there exists much debate on the relative roles of external and intrinsic drivers of canopy dynamics. Much of this debate may stem from the geographic differences in the environments of this well-adapted species. In the first part of this dissertation I used multispectral satellite imagery to help build a dataset of giant kelp canopy biomass dynamics along the coast of California across nearly three decades. We were then able to decompose this spatiotemporal matrix into orthogonal modes that allowed for the ranking of the most important environmental drivers of the kelp canopy: wave disturbance, seasonal nutrient supply, and the North Pacific Gyre Oscillation. We then used generalized additive models to determine the nonlinear effect shapes of each potential biomass driver. In the next chapter, we explored the physiology of the giant kelp canopy and found that photosynthetic pigment state and the chlorophyll *a* to carbon ratio (Chl:C) of the kelp canopy more closely resembles changes in available nitrate rather than changes in

available light at locations in southern California, while the reverse is true along the more nutrient-replete central California coastline. Temporally lagged Chl:C was positively related to changes in kelp biomass and net primary production along the periodically nutrient-limited southern California coast. These results open the possibility of estimating net primary production of giant kelp over large spatial and temporal scales using present and planned remote sensing technologies and the modeling of Chl:C based on well measured environmental variables. In the final chapter, we used hyperspectral imagery to examine the physiological condition of the giant kelp canopy over a variety of scales to identify and elucidate ecological processes related to external environmental drivers and demographics. We found that regional patterns of Chl:C were associated with large-scale fluctuations in sea surface temperature, and by extension ambient nutrient concentration. Local scale variability in Chl:C across a single kelp forest equaled the regional variability, implying that local scale processes also play a role in the physiological condition of this species. Local scale examples showed that canopy Chl:C was related to the date when kelp canopy first emerged, suggesting that demographic patterns in kelp frond age influence the local physiological condition and persistence of giant kelp canopy.

TABLE OF CONTENTS

LIST OF FIGURES

I. Introduction

Giant kelp (*Macrocystis pyrifera)* serves as the foundation species for an incredibly productive ecosystem whose consumptive and non-consumptive uses produce at least $250 million in revenue per year (Dayton 1984; Mann 2000; Leet et al. 2001). Giant kelp is usually encountered in its diploid sporophyte stage, which consists of a bundle of vine-like fronds anchored by a common holdfast. Blades develop along the length of the frond with a single pneumatocyst (gas bladder) at the base of each blade buoying the fronds to the surface where a dense canopy is formed. Individuals routinely attain lengths over 20 m and under ideal conditions can elongate at rates of up to 50 cm per day (Clendenning 1971). This high growth rate of giant kelp is coupled with a relatively short lifespan, leading to standing biomass turnover 6 to 7 times per year (Reed et al. 2008).

This variability in giant kelp biomass varies greatly across space and time. Recent studies have pioneered the use of remote sensing techniques to observe giant kelp canopy over scales that would have been infeasible or cost prohibitive otherwise (Cavanaugh et al. 2011). Bell, Cavanaugh, and Siegel (2015) used canopy biomass estimates from Landsat satellites to examine the differences in periodicity of giant kelp along the central and southern California coastlines. They found that the kelp forest canopy was dominated by a consistent seasonal cycle along the central coast, and by an intermittent interannual cycle in southern California.

This variability in giant kelp forest biomass is typically the result of the interplay of top-down forces from herbivory, bottom-up forces from the supply of nutrients, and disturbance from ocean swell (Harrold & Reed 1985; Gerard 1982; Zimmerman & Kremer 1984; Seymour et al. 1989; Graham et al. 1997). These processes can vary with location and time

1

and the relative strength of these forces may be understood by studying the spatial distribution of this species through time.

The growth of giant kelp thalli is fundamentally the result of available light and nutrients driving photosynthesis. While light availability to the canopy follows a highly predictable seasonal pattern, nutrient delivery to giant kelp forests is episodic with upwelling processes, internal waves, terrestrial storm runoff, and biological regeneration all driving important inputs (McPhee-Shaw et al. 2007, Hepburn & Herd 2005). As light and nutrient conditions change, giant kelp will vary cellular pigment levels to adjust to new photosynthetic demands (Kirk 1994). Under controlled light conditions, we would expect giant kelp to linearly increase its cellular concentrations of chlorophyll *a* as nutrient limitations were released, and that these increases in photosynthetic pigments will scale with growth rate (Laws & Bannister 1980; Shivji 1984).

Canopy density and production are known to vary across a single kelp forest. The growth rate of fronds near the outside edge of the forest was greater than fronds located in the interior of the forest when canopy density was high (Stewart et al. 2009). Canopy density is also variable across a single forest, with greater density in the center and in areas with a high proportion of hard bottom substrate (Cavanaugh et al. 2010). These differences in growth rate and density likely lead to differences in net primary production across the forest possibly affecting food web dynamics and carbon storage.

Aside from these external drivers of giant kelp variability and production are intrinsic factors like programmed senescence. Demographic patterns associated with progressive frond senescence have been shown to be a better predictor of frond loss than external environmental factors (Rodriguez et al. 2013). Blades also display a reduction in nitrogen

content and maximum photosynthetic capacity as they age, suggesting that there is a decrease in physiological condition in older, senescent fronds (Rodriguez et al. 2016).

In this dissertation I aim to answer the overarching question: What are the controls of giant kelp canopy dynamics across space and time? I attempt to do this by utilizing field, laboratory, and remote sensing techniques and by synthesizing the results to better understand how and why this species varies the way it does. I believe that taking advantage of broad temporal and spatial scales can help us better understand the relative roles of extrinsic and intrinsic drivers on this foundation species.

Literature Cited

Bell, T. W., K. C. Cavanaugh, and D. A. Siegel. 2015. Remote monitoring of giant kelp biomass and physiological condition: An evaluation of the potential for the Hyperspectral Infrared Imager (HyspIRI) mission. Remote Sens. Environ., **167**, 218–228. doi:10.1016/j.rse.2015.05.003

Cavanaugh, K., D. Siegel, B. Kinlan, D. Reed. 2010. Scaling giant kelp field measurements to regional scales using satellite observations. Marine Ecology Progress Series, **429**, 13-27.

Cavanaugh, K.C., Siegel, D.A., Reed, D.C. & Dennison, P.E. (2011) Environmental controls of giant-kelp biomass in the Santa Barbara Channel, California. Marine Ecology Progress Series, **429**, 1–17.

Clendenning, K. A. (1971) Photosynthesis and general development in *Macrocystis. The biology of giant kelp beds (*Macrocystis*) in California* (ed. by W.J. North), pp. 169–190. Beihefte zur Nova Hedwigia 32, Verlag von J. Cramer, Lehre, Germany.

Dayton, P. K., Currie, V., Gerrodette, T., Keller, B., Rosenthal, R., and D. Van Tresca. 1984. Patch dynamics and stability of southern CA kelp communities. Ecol. Monogr., **54**, 253-289.

Gerard, V.A. (1982) Growth and utilization of internal nitrogen reserves by the giant kelp *Macrocystis pyrifera* in a low-nitrogen environment. *Marine Biology*, **66**, 27–35.

Graham, M.H., Harrold, C., Lisin, S., Light, K., Watanabe, J.M. & Foster, M.S. (1997) Population dynamics of giant kelp *Macrocystis pyrifera* along a wave exposure gradient. *Marine Ecology Progress Series*, **148**, 269–279.

Harrold, C. & Reed, D.C. (1985) Food availability, sea urchin grazing, and kelp forest community structure. *Ecology*, **66**, 1160–1169.

Hepburn, C., and C. Hurd. 2005. Conditional mutualism between the giant kelp Macrocystis pyrifera and colonial epifauna. Marine Ecology Progress Series, **302**, 37–48.

Kirk, J. T. O. 1994. Light and Photosynthesis in Aquatic Ecosystems. Cambridge University Press. Cambridge, United Kingdom.

Laws, E., and T. Bannister. 1980. Nutrient and light-limited growth of Thalassiosira fluviatilis in continuous culture, with implications for phytoplankton growth in the ocean. Limnol. Oceanogr., **25**, 457–473.

Leet, W. S., Dewees, C. M., Klingbeil, R., and E. J. Johnson. 2001. California's living marine resources: A status report. State of CA Resources Agency and Fish and Game (593 pp.).

Mann, K.H. 2000. Ecology of coastal waters. Blackwell, Malden, Massachusetts, USA.

McPhee-Shaw, E.E., Siegel, D.A., Washburn, L., Brzezinski, M.A., Jones, J.L., Leydecker, A. & Melack, J. (2007) Mechanisms for nutrient delivery to the inner shelf: observations from the Santa Barbara Channel. *Limnology and Oceanography*, **52**, 1748–1766.

Reed, D. C., A. Rassweiler, and K. K. Arkema. 2008. Biomass rather than growth rate determines variation in net primary production by giant kelp. Ecology, **89**, 2493–2505. doi:10.1890/07-1106.1

Rodriguez, G.E., Rassweiler, A., Reed, D.C. & Holbrook, S.J. (2013) The importance of progressive senescence in the biomass dynamics of giant kelp (*Macrocystis pyrifera*). *Ecology*, **94**, 1848–1858.

Rodriguez, G.E., Reed, D.C. & Holbrook, S.J. 2016. Blade life span, structural investment, and nutrient allocation in giant kelp. Oecologia. doi:10.1007/s00442-016-3674-6

Seymour, R.J., Tegner ,M.J., Dayton, P.K. & Parnell, P.E. (1989) Storm wave induced mortality of giant kelp, *Macrocystis pyrifera*, in Southern California. *Estuarine, Coastal and Shelf Science*, **28**, 277–292.

Shivji, M. S. 1984. Physiological responses of juvenile *Macrocystis pyrifera* sporophytes (Phaeophyta) to environmental factors: light, nitrogen and the interaction of light and nitrogen. M.A. Thesis in Biology, University of California, Santa Barbara, 51 pp.

Stewart, H.L., Fram, J.P., Reed, D.C., Williams, S.L., Brzezinski, M.A., MacIntyre, S. & Gaylord, B. (2009) Differences in growth, morphology and tissue carbon and nitrogen of *Macrocystis pyrifera* within and at the outer edge of a giant kelp forest in California, USA. *Marine Ecology Progress Series*, **375**, 101–112.

Zimmerman, R.C. & Kremer, J.N. (1984) Episodic nutrient supply to a kelp forest ecosystem in Southern California. *Journal of Marine Research*, **42**, 591–604.

II. Geographical variability in the controls of giant kelp biomass dynamics[1]

Abstract

Aim Coastal marine environments experience a wide range of biotic and abiotic forces that can limit and punctuate the geographical range and abundance of species through time. Determining the relative strengths and nonlinear effects of these processes is vital to understanding the biogeographical structures of species. There has been an ongoing discussion concerning the relative importance of these processes in controlling the dynamics of giant kelp, an important structure-forming species on shallow reefs in the eastern Pacific. We use novel spatial time-series that span nearly three decades to determine the dominant drivers of giant kelp canopy biomass and the temporal and spatial scales over which they operate across the dominant range of the giant kelp in North America.

Location Near-shore areas from Año Nuevo, California, to the USA/Mexico border.

Methods We employed empirical orthogonal functions to elucidate the primary drivers of giant kelp canopy biomass across space and time and then fit generalized additive and linear models to determine the nonlinear effect and relative importance of each of these potential drivers along the *c.* 1500-km study region over a 25-year period.

Results Wave disturbance, nitrate availability and the state of the North Pacific Gyre Oscillation were the most important environmental predictors of giant kelp canopy biomass, explaining 24.5%, 12.7% and 6.1% of the variance, respectively. Environmental drivers of canopy biomass exhibited profound spatial differences in relative effect sizes. Nonlinear

---

effect shapes of each potential biomass driver were determined, which explained these spatial differences.

Main conclusions These large-scale analyses help to reconcile the local-scale conclusions of canopy biomass dynamics across the California coastline and show that these dynamics differ predictably in space and time in accordance with local and regional differences in environmental drivers. By characterizing the nonlinear effects of these drivers, we identified spatio-temporal patterns of processes that cannot be detected by remote sensing.

A. Introduction

The spatial distributions of organisms are driven by a combination of abiotic and biotic forces. Abiotic forces include climate, physical features of the environment and resource availability, whereas biotic forces involve the physiological performance of individuals as well as interactions within and between species. The influence of these processes may change in direction and magnitude across a wide range of spatial and temporal scales (Menge 1976). This variability has led to seemingly contradictory conclusions about the primary drivers of population abundance in a number of systems (reviewed in Power 1992).

Marine coastal environments experience a wide range of forces that can limit and punctuate the geographical range of an organism through time. For example, the distributions of two species of mussel (*Mytilus edulis* and *Mytilus trossulus*) in the north-eastern Atlantic can be partly attributed to physiological stress caused by aerial exposure, whereas interannual variations in ice floes can interrupt the density trends along the mussels' range (Tam & Scrosati 2011). Coastal environments also experience large-scale changes in ocean climate, which can fundamentally alter the distribution of a species. The

northward range expansion of Kellet's whelk (*Kelletia kelletii*; Herrlinger 1981) has been attributed to either warming sea-surface temperatures (SST), ocean circulation changes, or some combination of the two, across a biogeographical boundary, probably linked to El Niño events (Zacherl et al. 2003). The complexity of the coastal environment may further complicate the mixture of drivers on a species through time.

The coastline of California, USA, spans four shallow marine biogeographical regions (Hall 1964; Valentine 1966; Abbott & Hollenberg 1976; Blanchette et al. 2008), which are marked by differences in oceanographical environments: the Mendocinian, Montereyan, Southern Californian and Ensenadian regions. Winter storms in the North Pacific create large swell waves (> 4 m height) propagating from the north-west, whereas summer months see a mixture of smaller significant wave heights (< 3 m) from the south and north-west (O'Reilly & Guza 1993). The central coast of California (Año Nuevo to Point Conception) is more exposed to westerly and north-westerly swells as a result of its orientation, whereas the southern California mainland coast (Point Conception to the USA/Mexico border) has a range of wave exposures as a result of variable coastline orientations as well as the presence of the Californian Channel Islands. Coastal upwelling brings cold, nutrient-rich waters to the coastal shelf, and is strongest in the spring along the central coast, where nutrient-replete conditions persist for the entire year; upwelling is less intense and more intermittent in southern California, with low nutrient levels during the summer (Huyer 1983; McPhee-Shaw et al. 2007; Reed et al. 2011). Large-scale low-frequency climate cycles, such as the Pacific Decadal Oscillation and El Niño–Southern Oscillation (ENSO), affect conditions on interannual time-scales and can have large impacts on the biogeography and structure of marine communities (Dayton et al. 1999; Parnell et al. 2010).

The giant kelp, *Macrocystis pyrifera* (L.) C. Agardh, is a canopy-forming macroalga

that is widely distributed along the coast of California and serves as the foundation species

to a productive ecosystem (Graham et al. 2007). Giant kelp abundance in California is

extremely dynamic. It is highly susceptible to removal by ocean waves and it is not

uncommon for entire forests to be destroyed during a single storm (Seymour et al. 1989;

Graham et al. 1997; Edwards & Estes 2006); populations are, however, highly resilient, and

recovery to a full canopy often occurs within 1–2 years after local extinction (Reed et al.

2006). Individuals routinely attain lengths over 20 m and under ideal conditions can

elongate at rates of 50 cm per day (Clendenning 1971), which implies an important role for

nutrient supply to support these extreme growth rates (Jackson 1977; Gerard 1982;

Zimmerman & Kremer 1984; Stewart et al. 2009). Large areas of kelp forest can be

destroyed by grazing activities, primarily by sea urchins, which can denude large areas

(Harrold & Reed 1985), and the removal of the surface canopy by mechanized harvesters

causes additional reductions in kelp biomass (Kimura & Foster 1984; Foster & Schiel 2010).

Importantly, the processes thought to dominate the regulation of giant kelp forests can vary

with location and time (e.g. Jackson 1977; Dayton et al. 1992; Graham et al. 1997; Dayton

et al. 1999; Edwards 2004; Lafferty & Behrens 2005; Parnell et al. 2010; Cavanaugh et al.

2011; Reed et al. 2011). This suggests that the interplay between regulating forces may be

understood by studying the spatial distribution of this species through time.

Recent advances in satellite image analyses allow for frequent (monthly to seasonal),

long-term (25 years and continuing), high-resolution (30 m), large-scale (continental)

observations of giant kelp canopy biomass (Cavanaugh et al. 2011). These kelp data can be

combined with spatially explicit time-series of potential drivers to quantify the effects of

these drivers on giant kelp biomass across a wide geographical region. Here, we use these

data to explore how nutrients, wave disturbance, low-frequency oceanographical cycles,

human harvest and herbivory by sea urchins structure the spatial distribution of giant kelp

biomass through time, across the species' region of dominance on the rocky reefs of

California, USA. Our research focused on answering the following questions. (1) What are

the dominant drivers of kelp canopy biomass dynamics? (2) How does the relative

importance of these drivers vary across temporal scales of seasons to decades and spatial

scales of 500 m to 1500 km?

B. Methods

1. Giant kelp canopy biomass data

We studied giant kelp over its range of dominance along the coast of California, USA,

encompassing the area between Año Nuevo, California, and the USA/Mexico border (*c.*

1500 km of coastline; Fig. 1). Giant kelp canopy biomass was estimated at 30-m resolution

from January 1986 to January 2011 using multispectral Landsat 5 Thematic Mapper (TM)

satellite imagery following procedures developed by Cavanaugh et al. (2011). Briefly, each

Landsat 5 TM image was atmospherically corrected to standardize the radiometric signals

using 50 temporally stable ground control points (Furby & Campbell 2001). A multiple-end-

member spectral mixing analysis (Roberts et al. 1998) was applied to estimate the fractional

cover of two end-members, one static kelp end-member, and one of 30 seawater end-

members unique to each image. Kelp canopy biomass was estimated using the observed

relationship between diver-estimated kelp canopy biomass and Landsat pixel kelp fraction.

Cloud-free imagery allowed kelp biomass to be estimated every 1–2 months. Canopy

biomass determinations were binned into 500-m segments and interpolated onto a 3-month

time interval using piecewise cubic interpolation. The segment length of 500 m was chosen

to avoid spatial autocorrelation, because synchrony among canopy biomass observations

declines dramatically in the first 200 m of spatial separation (Cavanaugh et al. 2013). Each

segment was scaled as a proportion of the maximum (top 3%) canopy biomass observed

across the entire time-series to account for differences in the amount of kelp (referred to

here as 'proportional kelp biomass'). Coastline segments with zero canopy biomass in more

than 75% of seasons were removed from analysis, for a total of 723 coastal segments.

2. Physical, biological and harvest datasets

Spatio-temporal data were compiled for variables that are anticipated to describe

processes affecting giant kelp canopy biomass. Observations of significant wave height (H_s)

were assessed using the National Buoy Data Center's (NBDC; http://www.ndbc.noaa.gov/)

Harvest platform and Harvest buoy, located *c.* 30 km offshore from Point Conception (Fig.

1a). The Harvest platform collected hourly observations of H_s and period from January 1987

to April 1999, and the Harvest buoy collected H_s, period and direction from March 1998 to

present. Records from the platform and buoy were combined to form a single H_s time-series

at the Harvest platform. Data from the Coastal Data Information Program's (CDIP;

http://cdip.ucsd.edu/) nowcast wave-propagation model were used to assess spatial

variations in H_s. CDIP provided hourly estimates of H_s at a depth of 10 m from June 1998 to

November 2011 for the entire domain at 800-m spatial resolution. Each coastline segment

was assigned a seasonal maximum H_s from the closest CDIP wave-model pixel. To

complete the record, H_s values were statistically modeled using a generalized additive model

from observations of H_s and dominant period from the Harvest platform, and a probability

distribution of swell direction.

Surface nitrate concentrations were estimated using sea-surface temperature (SST) records and the observed relationship between ocean temperature and nitrate concentration following Zimmerman & Kremer (1984). A continuous time series of SST is available near the center of the domain from the NBDC Point Arguello buoy (hourly from 1986 to 2011) located *c.* 20 km offshore from Point Arguello, and at each site from the Advanced Very High Resolution Radiometer (AVHRR; http://www.ncdc.noaa.gov/sst/) satellite images from 1987 to 2011. Seasonal mean nitrate values were determined for each coastline segment.

Three oceanographical climate indices were also used in this study: the North Pacific Gyre Oscillation (NPGO; http://www.o3d.org/npgo), Pacific Decadal Oscillation (PDO; http://jisao.washington.edu/pdo), and the Multivariate ENSO index (MEI; http://www.esrl.noaa.gov/psd/enso/mei). These climate oscillations fluctuate over interannual to decadal time-scales and are known to have large effects on the California Current system in general and on giant kelp populations in particular (Dayton & Tegner 1984; Di Lorenzo et al. 2008; Parnell et al. 2010). Positive values in the NPGO index correspond with stronger wind-driven upwelling, which leads to greater nutrient concentrations along the California coast, whereas positive MEI values are associated with El Niño conditions, with decreases in wind-driven upwelling, warmer surface waters and nutrient-poor conditions. Positive PDO values indicate warmer SST, and nutrient-poor conditions along the western coast of the contiguous United States. All environmental variables were lagged by one season, because wave disturbance and changes in nutrient concentrations were expected to affect giant kelp canopy biomass over relatively short time-scales.

Kelp canopy harvest records for every California Department of Fish and Wildlife administrative bed harvested by ISP Alginates were available from 1991 until harvesting ended in 2006 (Reed 2010). In order to calculate the amount of harvest effort in each coastline segment, the harvested kelp was apportioned to each segment based on the proportion of total kelp canopy biomass of the segment within the administrative bed. The amount of kelp harvested was then divided by the total segment canopy kelp biomass in the season prior to obtain a measure of harvest effort, ranging from zero (no harvest) to one (complete harvest of the kelp canopy).

Densities of purple and red sea urchins (*Strongylocentrotus purpuratus* and *Mesocentrotus franciscanus*, respectively) were measured at a small fraction of the sites (Kenner et al. 2013; Kushner et al. 2013; Reed 2013). Annual sea urchin density surveys started between 1982 and 2001 for the 45 sites with records long enough to be included in the analyses.

3. Empirical orthogonal function analysis

Dominant drivers of kelp canopy biomass were identified using an empirical orthogonal function (EOF) analysis (Lorenz 1956). EOF analysis compresses a set of correlated time-series into a ranked set of uncorrelated ones, each with a spatial map illustrating the loadings for that mode. EOF modes were ordered by the fraction of variance explained. Here, we decomposed the space–time distribution of kelp canopy biomass into a ranked set of orthogonal spatial loadings and temporal amplitude functions. Each EOF mode described a known fraction of the total variance in kelp canopy biomass and collectively accounted for the covariability of the space–time biomass distribution. A physical interpretation for each mode was made by examining the relationships between the EOF spatial loadings and

13

temporal amplitude functions with the different environmental parameters. Pearson product-moment correlation coefficients between environmental variables and the EOF temporal amplitude function indicate how closely the variable matched the changes in direction and magnitude of the amplitude function through time, whereas correlations with the EOF spatial loadings indicate how closely the variable matched the magnitude of the loadings in space. Significance between EOF outputs and environmental variables was tested using permutation tests with 1000 permutations.

4. Generalized additive model analysis

A generalized additive model (GAM) was applied to each coastal segment in the study domain in order to determine the dynamic relationships between kelp canopy biomass and the environmental drivers. The general concept of GAMs is that a response variable (e.g. kelp biomass) can be modeled as the sum of non-linear functions of different predictor variables (Hastie & Tibshirani 1990). The underlying relationship between each predictor variable and kelp canopy biomass was determined using thin-plate penalized regression splines, which adds penalties to wiggly functions to avoid overfitting (Wood & Augustin, 2002). The weight of these penalties was optimized using generalized cross-validation, which minimizes the root mean square error between the fit and data points. Optimal model form was selected by minimizing the Akaike information criterion, which helps balance the complexity of the model versus the goodness of fit. We used the R package MGCV to implement all GAMs with $\alpha = 0.05$ (Version 1.8-6; Wood 2006). Standardized coefficients of each significant predictor were estimated at each coastline segment by using a multiple linear regression to fit each z-score scaled (mean, 0; variance, 1) variable to scaled proportional kelp canopy biomass.

The environmental correlates identified in the EOF analysis – maximum significant wave height, mean nitrate concentration and the value of the NPGO – were used as predictors in local GAMs for each coastline segment all lagged in time by one season (log link function; Gaussian error structure). Harvest effort was also added as a predictor to the model for the known harvested coastline segments, and a kelp occupancy term (the proportion of kelp canopy biomass in the previous season) allowed kelp canopy biomass to respond according to prior occupancy at each segment. Sea urchin density was added to the predictors already included in the GAM at sites with urchin observations.

C. Results

1. Spatio-temporal variability in kelp biomass

Giant kelp canopy biomass was variable throughout the study area with mean seasonal biomass per 500 m coastline segment ranging between 1000 and 1.37×10^6 kg wet mass (Fig. 1a,b). The mean coefficient of variation (CV) averaged across all measured seasons was 1.4 for the entire study region and rarely dropped below 1 in any 500-m coastline segment, demonstrating the high variability of giant kelp canopy biomass during the 25-year study period (Fig. 1c). Marked spatial differences in CV were found between different sides of islands and between protected and exposed areas on the mainland. The study region supported a mean kelp canopy biomass of 1.39×10^8 kg, which ranged from a maximum of 4.14×10^8 kg in the autumn of 2005 to a minimum of 4.74×10^6 kg in the spring of 1998, following winter storms during a large El Niño episode.

2. Diagnosing correlates of kelp biomass dynamics

EOF spatial loadings and temporal amplitude functions were linearly correlated with

environmental variables, revealing the dominant environmental processes that drive variations in giant kelp biomass (Table 1). The first mode explained 24.5% of the variance and its temporal variations displayed a clear seasonal pattern, with positive values in the winter and spring and negative values in the summer and autumn. This amplitude time-series was significantly correlated with maximum H_s during the previous season from the Harvest buoy ($r = 0.59$; $P < 0.001$; Fig. 2a). The spatial loadings of the first mode revealed large negative values for the central coast and values near zero throughout much of the southern California with exceptions on the exposed sides of the Channel Islands (Fig. 2b). Mean seasonal maximum H_s along the California coast from the CDIP H_s model was strongly correlated with the spatial loadings ($r = -0.69$; $P < 0.001$), implying that swells have a large negative effect on kelp biomass throughout the central coast and much less of an impact in southern California, except for exposed sites. The loadings were significantly correlated with site-specific maximum H_s in both time and space; the overwhelmingly negative spatial loadings across the study area were indicative of negative effects on kelp biomass during winter and spring, the seasons in which the temporal amplitude function of the first EOF was positive.

The second EOF mode explained 12.7% of the biomass variance and its temporal amplitude function displayed a strong seasonal pattern (Fig. 2c). This amplitude time-series was significantly correlated with mean nitrate concentrations in the surface waters during the previous season from the Point Arguello buoy ($r = 0.49$; $P < 0.001$), with positive amplitude during winter and spring periods of high nitrate, and negative mode amplitudes during summer and autumn periods of low nitrate. The second mode spatial loadings displayed positive values in southern California and values near or below zero along the

16

central coast (Fig. 2d). These loadings were significantly correlated with all of the spatial variables ($P < 0.001$), but only mean seasonal nitrate along the California coast was consistent with the positive spatial loadings throughout most of the study area ($r = -0.73$; $P < 0.001$). This correlation suggests that higher nitrate concentrations correspond to positive kelp biomass levels in areas with lower mean nitrate (e.g. southern California).

The third mode explained 6.1% of the biomass variance and the temporal amplitude function displayed interannual changes that were significantly correlated with the NPGO index during the previous season ($r = 0.44$; $P < 0.001$; Fig. 2e). The third mode spatial loadings showed the highest positive values along the south-eastern corner of southern California, San Clemente and Santa Catalina Islands, which are the most oligotrophic regions of the study region, and the northern half of the central coast (Fig. 2f). Positive values of NPGO are related to periods of high nitrate availability (Di Lorenzo et al. 2008). The spatial loadings were significantly correlated with the percentage of seasons with a mean surface nitrate concentration below 1 μmol L^{-1} ($r = 0.39$; $P < 0.001$), the minimum threshold concentration needed to sustain kelp growth (Zimmerman & Kremer 1984).

3. Modeling drivers of biomass dynamics

A total of 723 coastline segments (500 m each) were analyzed using individual GAMs. The R^2 of the individual segment models ranged from 0.09 to 0.79 (Fig. 3a), with an ensemble mean R^2 equal to 0.41. Standardized coefficients of each significant predictor were estimated for each coastline segment using a linear model to fit each variable to proportional kelp biomass (Fig. 3b–g; Table 2). At the 470 southern California coastline segments, maximum H_s was the best predictor at 36.8%, mean nitrate at 28.9%, NPGO at 5.3%, kelp harvest at 9.2%, and no significant predictor at 19.8% of the sites. Of the 253 central

California segments, maximum H_s was the best predictor at 91.7%, mean nitrate at 5.5%, no significant predictor at 1.6%, and NPGO at 1.2% of the sites. Sea urchin density had the greatest magnitude-standardized coefficient at 9 of the 36 southern California sites and none of the central California sites, although southern California segments where sea urchin density was measured had lower median winter wave heights (0.94 m) than the southern California as a whole (1.23 m; $P < 0.001$; Wilcoxon rank-sum test).

The mean additive effect of each predictor variable on proportional kelp biomass was found by averaging the individual effect relationships of each predictor from all coastal segments where the predictor was statistically significant (Fig. 4). These plots show the mean direction and magnitude of each predictor on kelp biomass. The mean relationship with seasonal maximum H_s was nonlinear and negative and showed the largest magnitude of effect, with larger swell having a negative effect at maximum $H_s > 2.5$ m. The mean relationship with nitrate showed a negative effect between values of 0 and 2 μmol L^{-1} and positive effects at concentrations above about 6 μmol L^{-1}. The NPGO index displayed a nonlinear effect relationship with biomass, with larger positive index values showing an increasing positive effect. Kelp occupancy showed a positive mean relationship with biomass, with greater biomass in the previous season showing positive effects at values greater than 0.1 proportional biomass. Kelp harvesting showed a small positive effect at values below 0.8 harvest effort, whereas increases in harvesting effort beyond this point had a negative effect. Sea urchin density showed negative, but diminishing, additive effects on kelp biomass as urchin density increased.

D. Discussion

1. Spatial heterogeneity in drivers of canopy biomass dynamics

Understanding how consumer pressure, resource availability and disturbance control the

dynamics of plant and algal populations is challenging, because the roles of these processes

can vary in space and time (Estes & Palmisano 1974; Menge 1976; Hunter & Price 1992;

Reed et al. 2011). Here, we have used EOF analysis and nonlinear additive modeling to

identify and quantify the relative strengths of these population drivers. For the California

coastline as a whole, wave disturbance was the dominant correlate of kelp canopy biomass,

followed by nitrate availability and the state of the NGPO. However, the relative importance

of these factors varied spatially. Studies that focus on one or a few sites may identify how

these factors relate to one another locally, but will miss how these relative effects vary

spatially. By examining hundreds of local coastline segments across many hundreds of

kilometers and over many generations, a comprehensive understanding of how these factors

contribute to the canopy dynamics of giant kelp can be achieved.

Wave disturbance events are larger and more frequent along the central coast than

the more protected southern California coastline, and thus represent a greater and more

consistent driver of biomass along wave-exposed coastline (Reed et al. 2011). Wave

disturbance showed an increasingly negative effect on kelp biomass at $H_s > 2.5$ m (Fig. 4).

We saw a clear increase in the magnitude of the surface wave disturbance coefficient north

of Point Conception, where the mean maximum winter H_s among all central coast sites was

3.3 m. Wave disturbance can also have a large effect on kelp biomass throughout southern

California, such as the large storm events associated with El Niño episodes (Dayton &

Tegner 1984, although large wave events are less frequent in southern California (7.7

seasonal maximum events above 2.5 m per coastline segment in southern California, versus

39.7 in central California during the period of study) and thus explained a smaller amount of variation in kelp dynamics in southern California.

The frond elongation rate is reduced at low nitrate concentrations, and surface water nitrate concentrations (as estimated from SST) showed a significant positive relationship with canopy biomass at 49% of the sites across the entire study region (Zimmerman & Kremer 1984). It was, however, the dominant correlate only at protected sites along the central coast or in southern California, where wave disturbance is reduced. Mean nitrate displayed negative effects on biomass at low concentrations and positive effects at high concentrations, with little effect at intermediate levels (2–6 μmol L^{-1}; Fig. 4). Although canopy persistence depends on many factors (Rodriguez et al. 2013), in the absence of periodic removal by disturbance, kelp forests can maintain a canopy throughout the year and may be primarily influenced by interannual cycles of nutrient availability (Parnell et al. 2010). Periods of high nutrient concentrations have been associated with increased kelp growth (Gerard 1982; Zimmerman & Kremer 1984; Stewart et al. 2009), and the shoaling of high-density, nutrient-rich waters over the inner shelf explains much of the interannual variation in kelp plant density in the southern end of the study area (Parnell et al. 2010). Interannual variation in nutrient concentrations is associated with changes in the state of the NPGO, which operates over interannual timescales and is characterized by increased upwelling and horizontal advection of cool waters from the north, extending to the southern Channel Islands (Di Lorenzo et al. 2008). These increased incursions of cold, nutrient-rich waters into the Southern California Bight may be partly responsible for the episodic dynamics of kelp forests in regions that are usually defined by oligotrophic conditions, such as San Clemente and Santa Catalina islands and the lower portion of the southern California

mainland coast (Kopczak et al. 1991; Di Lorenzo et al. 2008). Positive values of the NPGO index display positive effects on kelp biomass, with values above 1.4 having increased positive effects (Fig. 4). Although El Niño variations were not primarily correlated with any of the kelp biomass EOFs, the wave disturbance and nutrient conditions typical of these events may have been partly explained within the first three EOF temporal amplitude functions, where interannual variation in the strength of each seasonal cycle is evident, especially during strong El Niño episodes.

Top-down effects by grazing sea urchins have been hypothesized to have increased in the past two centuries as a result of human-induced alteration of kelp forest food webs. This resulted from the extirpation of sea otters by hunting and overfishing of predatory species of fish and invertebrates, and may have led to increased abundances of sea urchins and other kelp grazers (Estes & Palmisano 1974). Our results show that higher sea urchin densities were associated with decreases in kelp canopy biomass and sea urchin density was the dominant correlate at 25% of the sites with long-term sea urchin records in southern California. For central-coast segments where urchin observations were available, sea urchin density was 20 times lower than in southern California. At two of the three central coast segments where the sea urchin density was significantly correlated with kelp biomass, a positive relationship was observed, indicating that increased kelp may be supporting greater numbers of sea urchins. This reinforces the notion that the top-down grazing by sea urchins is an important local-scale driver of kelp biomass in southern California, but not central California in areas where sea otters are prevalent (VanBlaricom & Estes 1988; Reed et al. 2011).

2. Addressing unknown drivers

The modeling of the biogeographical structure of a species requires an understanding of the relative importance of the causative environmental drivers (Fenberg et al. 2014). Remotely sensed and modeled datasets can provide insight into the mechanisms that cause populations to fluctuate at different spatial and temporal scales. Data for some potentially important covariates, such as sea urchin density, require time-consuming diver surveys, however, which limits their spatial and temporal extent. Furthermore, records for some predictor variables, such as kelp harvest, may not extend throughout the entire time-series. The lack of comprehensive data on such drivers limits our ability to fully understand the processes that control the dynamics and distribution of the species we study.

Here, we use observations from a time-series of giant kelp canopy biomass and its major environmental drivers (e.g. wave heights, nitrate concentrations and oceanographical conditions) to model kelp biomass dynamics across a 1500-km stretch of the California coast. Sustained departures between these model predictions and observations may indicate the occurrence of unknown processes that have a significant impact on kelp biomass. An example can be seen at the Carpinteria kelp forest near Santa Barbara, California, where the time-series of sea urchin density was not included in the model (Fig. 5). From 1998 to 2005, kelp canopy was completely absent from the Carpinteria coastline segment, but the model predicted multiple cycles of kelp growth and removal during this absence. Sea urchin abundance was especially high during this absence of kelp canopy, suggesting that top-down grazing pressure overwhelmed the effects of wave disturbance and nutrient availability during this period.

The detection of model mismatch throughout the time-series may provide a path for

the elucidation of unknown or poorly-known environmental drivers. By relating the degree and duration of model–data mismatches to predictors measured at local-scale sites, one can infer where and when additional forces are likely to be dominant. This can lead to directed sampling efforts or the inference of the progression of drivers through time and space, providing additional insights into the importance of unknown factors in controlling populations.

Understanding the spatial heterogeneity of processes that exert control over populations remains a major focus for landscape ecology and biogeography (Turner 1989). Our results demonstrate the importance of multiscale analyses of ecosystem dynamics. A variety of known and unknown environmental and biotic forces interact to structure these systems, which vary not only through time, but also in space. This spatial variability has the potential to lead to conflicting conclusions concerning the relative importance of different factors, as many studies investigating biomass and population dynamics are conducted in relatively small plots, in a small portion of a species' geographical range. Large-scale, long-term, persistently sampled datasets allow for a comprehensive characterization of spatial and temporal variability and the factors that influence this variability. Results from such studies inform not only what has happened in the past, but allow one to infer how future changes in drivers may disproportionately affect certain locations or regions.

E. Chapter Acknowledgements

F. Literature Cited

Abbott, I.A. & Hollenberg, G.J. (1976) *Marine algae of California*. Stanford University Press, Stanford, CA.

Blanchette, C.A., Miner, C.M., Raimondi, P.T., Lohse, D., Heady, K.E.K. & Broitman, B.R. (2008) Biogeographical patterns of rocky intertidal communities along the Pacific coast of North America. *Journal of Biogeography*, **35**, 1593–1607.

Cavanaugh, K.C., Siegel, D.A., Reed, D.C. & Dennison, P.E. (2011) Environmental controls of giant-kelp biomass in the Santa Barbara Channel, California. *Marine Ecology Progress Series*, **429**, 1–17.

Cavanaugh, K.C., Kendall, B.E., Siegel, D.A., Reed, D.C., Alberto, F. & Assis, J. (2013) Synchrony in dynamics of giant kelp forests is driven by both local recruitment and regional environmental controls. *Ecology*, **94**, 499–509.

Clendenning, K.A. (1971) Photosynthesis and general development in *Macrocystis*. *The biology of giant kelp beds (*Macrocystis*) in California* (ed. by W.J. North), pp. 169–190. Beihefte zur Nova Hedwigia 32, Verlag von J. Cramer, Lehre, Germany.

Dayton, P.K. & Tegner, M.J. (1984) Catastrophic storms, El Niño, and patch stability in a southern California kelp community. *Science*, **224**, 283–285.

Dayton, P.K., Tegner, M.J., Parnell, P.E. & Edwards, P.B. (1992) Temporal and spatial patterns of disturbance and recovery in a kelp forest community. *Ecological Monographs*, **62**, 421–445.

Dayton, P.K., Tegner, M.J., Edwards, P.B. & Riser, K.L. (1999) Temporal and spatial scales of kelp demography: the role of oceanographic climate. *Ecological Monographs*, **69**, 219–250.

Di Lorenzo, E., Schneider, N., Cobb, K.M., Franks, P.J.S., Chhak, K., Miller, A.J., McWilliams, J.C., Bograd, S.J., Arango, H., Curchitser, E., Powell, T.M. & Rivière, P. (2008) North Pacific Gyre Oscillation links ocean climate and ecosystem change. *Geophysical Research Letters*, **35**, L08607.

Edwards, M.S. (2004) Estimating scale-dependency in disturbance impacts: El Niños and giant kelp forests in the northeast Pacific. *Oecologia*, **138**, 436–447.

Edwards, M.S. & Estes, J.A. (2006) Catastrophe, recovery and range limitation in NE Pacific kelp forests: a large-scale perspective. *Marine Ecology Progress Series*, **320**, 79–87.

Estes, J.A. & Palmisano, J.F. (1974) Sea otters: their role in structuring nearshore communities. *Science*, **185**, 1058–1060.

Fenberg, P.B., Menge, B.A., Raimondi, P.T. & Rivadeneira, M.M. (2014) Biogeographic structure of the northeastern Pacific rocky intertidal: the role of upwelling and dispersal to drive patterns. *Ecography*, **37**, 1–13.

Foster, M.S. & Schiel, D.R. (2010) Loss of predators and the collapse of southern California kelp forests (?): alternatives, explanations and generalizations. *Journal of Experimental Marine Biology and Ecology*, **393**, 59–70.

Furby S.L. & Campbell N. a. (2001) Calibrating images from different dates to "like-value" digital counts. *Remote Sensing of Environment*, **77**, 186–196.

Gerard, V.A. (1982) Growth and utilization of internal nitrogen reserves by the giant kelp *Macrocystis pyrifera* in a low-nitrogen environment. *Marine Biology*, **66**, 27–35.

Graham, M.H., Harrold, C., Lisin, S., Light, K., Watanabe, J.M. & Foster, M.S. (1997) Population dynamics of giant kelp *Macrocystis pyrifera* along a wave exposure gradient. *Marine Ecology Progress Series*, **148**, 269–279.

Graham, M.H., Vásquez, J.A. & Buschmann, A.H. (2007) Global ecology of the giant kelp *Macrocystis*: from ecotypes to ecosystems. *Oceanography and Marine Biology: an Annual Review*, **45**, 39–88.

Hall, C.A. (1964) Shallow-water marine climates and molluscan provinces. *Ecology*, **45**, 226–234.

Harrold, C. & Reed, D.C. (1985) Food availability, sea urchin grazing, and kelp forest community structure. *Ecology*, **66**, 1160–1169.

Hastie, T.J. & Tibshirani, R.J. (1990) *Generalized additive models*. Chapman & Hall, London, UK.

Herrlinger, T.J. (1981) Range extension of *Kelletia kelletii*. *The Veliger*, **24**, 78.

Hunter, M.D. & Price, P.W. (1992) Playing chutes and ladders: heterogeneity and the relative roles of bottom-up and top-down forces in natural communities. *Ecology*, **73**, 724–732.

Huyer, A. (1983) Coastal upwelling in the California current system. *Progress in Oceanography*, **12**, 259–284.

Jackson, G.A. (1977) Nutrients and production of giant kelp, *Macrocystis pyrifera*, off southern California. *Limnology and Oceanography*, **22**, 979–995.

Kenner, M.C., Estes, J.A., Tinker, M.T., Bodkin, J.L., Cowen, R.K., Harrold, C. Hatfield, B.B., Novak, M., Rassweiler, A. & Reed, D.C. (2013) A multi-decade time series of kelp forest community structure at San Nicolas Island, California (USA). *Ecology*, **94**, 2654.

Kimura, R.S. & Foster, M.S. (1984) The effects of harvesting *Macrocystis pyrifera* on the algal assemblage in a giant kelp forest. *Hydrobiologia*, **116–117**, 425–428.

Kopczak, C.D., Zimmerman, R.C. & Kremer, J.N. (1991) Variation in nitrogen physiology and growth among geographically isolated populations of the giant kelp, *Macrocystis pyrifera* (Phaeophyta). *Journal of Phycology*, **27**, 149–158.

Kushner, D.J., Rassweiler, A., McLaughlin, J.P. & Lafferty, K.D. (2013) A multi-decade time series of kelp forest community structure at the California Channel Islands. *Ecology*, **94**, 2655.

Lafferty, K.D. & Behrens, M.D. (2005) Temporal variation in the state of rocky reefs: does fishing increase the vulnerability of kelp forests to disturbance? *Proceedings of the Sixth California Islands Symposium* (ed. by D.K. Garcelon *and C.A.* Schwemm)*, pp. 499–508, Ventura, CA, December 1 – 3, 2003. National Park Service technical publication.*

Lorenz, E.N. (1956) *Empirical orthogonal functions and statistical weather prediction.* Technical Report Statistical Forecast Project Report 1. Department of Meteorology, Massachusetts Institute of Technology, Cambridge, MA.

McPhee-Shaw, E.E., Siegel, D.A., Washburn, L., Brzezinski, M.A., Jones, J.L., Leydecker, A. & Melack, J. (2007) Mechanisms for nutrient delivery to the inner shelf: observations from the Santa Barbara Channel. *Limnology and Oceanography*, **52**, 1748–1766.

Menge, B.A. (1976) Organization of the New England rocky intertidal community: role of predation, competition, and environmental heterogeneity. *Ecological Monographs*, **46**, 355–393.

O'Reilly, W.C. & Guza, R.T. (1993) A comparison of two spectral wave models in the Southern California Bight. *Coastal Engineering*, **19**, 263–282.

Parnell, P.E., Miller, E.F., Lennert-Cody, C.E., Dayton, P.K., Carter, M.L. & Stebbins, T.D. (2010) The response of giant kelp (*Macrocystis pyrifera*) in southern California to low-frequency climate forcing. *Limnology and Oceanography*, **55**, 2686–2702.

Power, M. (1992) Top-down and bottom-up forces in food webs: do plants have primacy? *Ecology*, **73**, 733–746.

Reed, D.C. (2010) *SBCLTER: reef: historical kelp database for giant kelp (*Macrocystis pyrifera*) biomass in California and Mexico.* Santa Barbara Coastal LTER. doi:10.6073/pasta/25d83a6ba159e5490a5f6a687a7e0d2b.

Reed, D.C. (2013) *SBCLTER: reef: kelp forest community dynamics: invertebrate and algal density*. Santa Barbara Coastal LTER. doi:10.6073/pasta/58474c2327f5e1399e3ef2eef40529cd.

Reed, D.C., Kinlan, B.P., Raimondi, P.T., Washburn, L., Gaylord, B. & Drake, P.T. (2006) A metapopulation perspective on patch dynamics and connectivity of giant kelp. *Marine metapopulations* (ed. by J.P. Kritzer and P.F. Sale), pp. 353–386. Academic Press, San Diego, CA.

Reed, D.C., Rassweiler, A., Carr, M.H., Cavanaugh, K.C., Malone, D.P. & Siegel, D.A. (2011) Wave disturbance overwhelms top-down and bottom-up control of primary production in California kelp forests. *Ecology*, **92**, 2108–2116.

Roberts, D.A., Gardner, M., Church, R., Ustin, S., Scheer, G. & Green, R.O. (1998) Mapping chaparral in the Santa Monica Mountains using multiple endmember spectral mixture models – II. Environmental influences on regional abundance. *Remote Sensing of Environment,* **65**, 267–279.

Rodriguez, G.E., Rassweiler, A., Reed, D.C. & Holbrook, S.J. (2013) The importance of progressive senescence in the biomass dynamics of giant kelp (*Macrocystis pyrifera*). *Ecology*, **94**, 1848–1858.

Seymour, R.J., Tegner ,M.J., Dayton, P.K. & Parnell, P.E. (1989) Storm wave induced mortality of giant kelp, *Macrocystis pyrifera*, in Southern California. *Estuarine, Coastal and Shelf Science*, **28**, 277–292.

Stewart, H.L., Fram, J.P., Reed, D.C., Williams, S.L., Brzezinski, M.A., MacIntyre, S. & Gaylord, B. (2009) Differences in growth, morphology and tissue carbon and nitrogen of *Macrocystis pyrifera* within and at the outer edge of a giant kelp forest in California, USA. *Marine Ecology Progress Series*, **375**, 101–112.

Tam, J.C. & Scrosati, R.A. (2011) Mussel and dogwhelk distribution along the north-west Atlantic coast: testing predictions derived from the abundant-centre model. *Journal of Biogeography*, **38**, 1536–1545.

Turner, M.G. (1989) Landscape ecology: the effect of pattern on process. *Annual Review of Ecology and Systematics*, **20**, 171–197.

Valentine, J.W. (1966) Numerical analysis of marine molluscan ranges on extratropical northeastern Pacific shelf. *Limnology and Oceanography*, **11**, 198–211.

VanBlaricom, G.R. & Estes, J.A. (1988) *The community ecology of sea otters*. Springer, New York.

Wood, S.N. (2006) *Generalized additive models: an introduction with R.* Texts in Statistical Science. Chapman & Hall/CRC, Boca Raton, FL.

Wood, S.N. & Augustin, N.H. (2002) GAMs with integrated model selection using penalized regression splines and applications to environmental modelling. *Ecological Modelling*, **157**, 157–177.

Zacherl, D., Gaines, S.D. & Lonhart, S.I. (2003) The limits to biogeographical distributions: insights from the northward range extension of the marine snail, *Kelletia kelletii* (Forbes, 1852). *Journal of Biogeography*, **30**, 913–924.

Zimmerman, R.C. & Kremer, J.N. (1984) Episodic nutrient supply to a kelp forest ecosystem in Southern California. *Journal of Marine Research*, **42**, 591–604.

Table 2.1. Correlation coefficients between empirical orthogonal function temporal mode amplitude functions/spatial loadings and physical and oceanographical variables. Mean nitrate concentrations estimated from sea-surface temperature. Bold values are significant at $P < 0.05$.

Temporal amplitude function	Proportion of variance	Max. significant wave height (H_s)	Mean nitrate	North Pacific Gyre Oscillation index	Pacific Decadal Oscillation index	Multivariate ENSO index	Southern Oscillation index
1	24.5%	**0.592**	**0.358**	0.089	−0.188	0.025	−0.018
2	12.7%	0.105	**0.490**	0.013	−0.021	−0.142	0.187
3	6.1%	−0.066	−0.115	**0.436**	−0.028	**−0.354**	−0.025

Spatial loadings	Spatial max. H_s	Spatial mean nitrate	% < 1 μmol L^{-1} nitrate
1	**−0.687**	**−0.762**	**0.725**
2	**−0.648**	**−0.727**	**0.655**
3	0.088	**−0.244**	**0.391**

Table 2.2. Mean *z*-score standardized coefficient, for each tested environmental predictor of giant kelp canopy biomass, across all significant coastline segments and well as the percentage of coastline segments where the predictor was significant at α = 0.05. Mean nitrate concentrations estimated from sea-surface temperature. Sea urchin density was investigated at 45 of the 723 sites.

Predictor	Mean model coefficient	Proportion significant
Max. significant wave height	−0.421	67.1%
Mean nitrate	0.223	49.0%
North Pacific Gyre Oscillation index	0.085	21.7%
Kelp occupancy	0.384	88.7%
Harvest effort	−0.003	18.3%
Sea urchin density	−0.212	42.2%

Figure 2.1. (a) Mean giant kelp canopy biomass at every 500-m coastline segment across every measured season, from 1986 to 2011, along the coast of California, USA. The star shows the approximate location of the Harvest platform and buoy, Point Arguello buoy, and Point Conception (plate carrée projection). (b) Mean kelp canopy biomass plotted as lines running from south to north, including the Channel Islands inside the horizontal dashed lines. Site locations for each island start at the location of the arrow and proceed clockwise around the island. (c) The coefficient of variation (CV) of kelp canopy biomass at each coastline segment across all seasons and years.
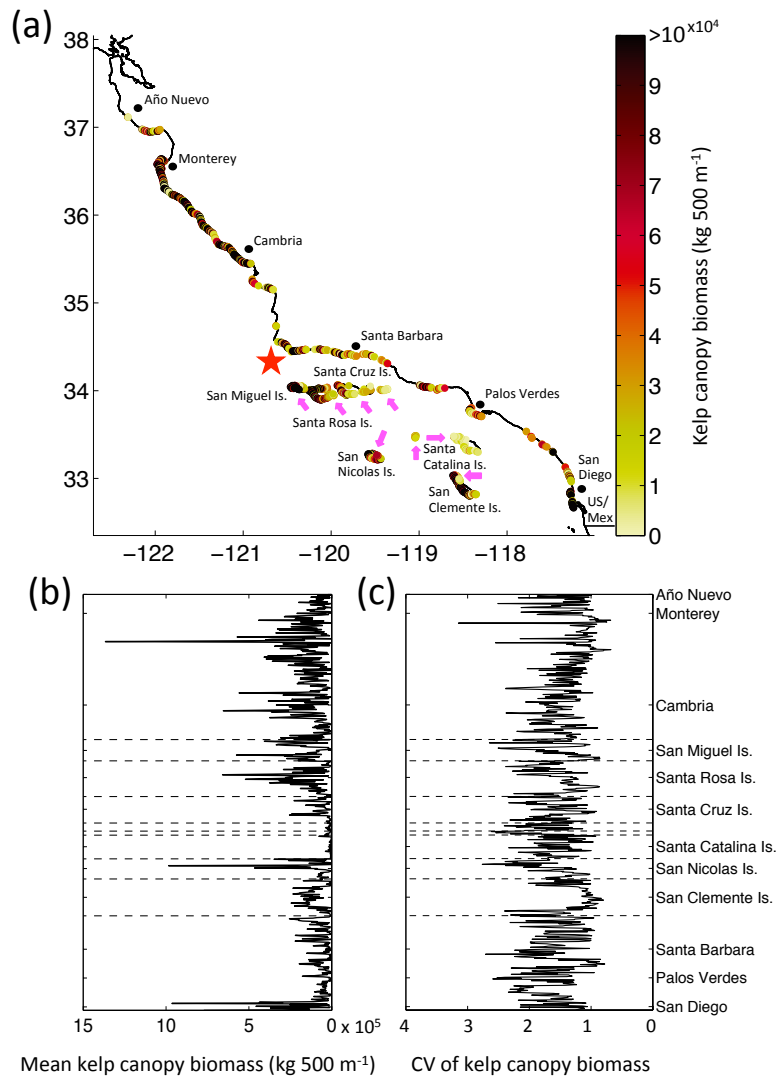
Figure 2.2. (a) First (a), second (c) and third (e) temporal amplitude functions from the empirical orthogonal function analysis of the giant kelp canopy biomass dynamics along the coast of California, USA. Spatial time series as solid lines and temporally correlated physical and oceanographical variables as dashed lines, (a) maximum significant wave height (H_s), (c) mean nitrate, and (e) North Pacific Gyre Oscillation index. Mean nitrate concentrations estimated from sea-surface temperature. These three modes explain 24.5%, 12.7% and 6.1% of the total variance, respectively. First (b), second (d), and third (f) spatial loadings as solid lines with spatially correlated environmental variables as dashed lines, (b) mean seasonal maximum H_s, (d) mean nitrate, and (f) percentage of seasons where mean nitrate < 1 µmol L^{-1}. All correlations shown are significant at $P < 0.001$.

33
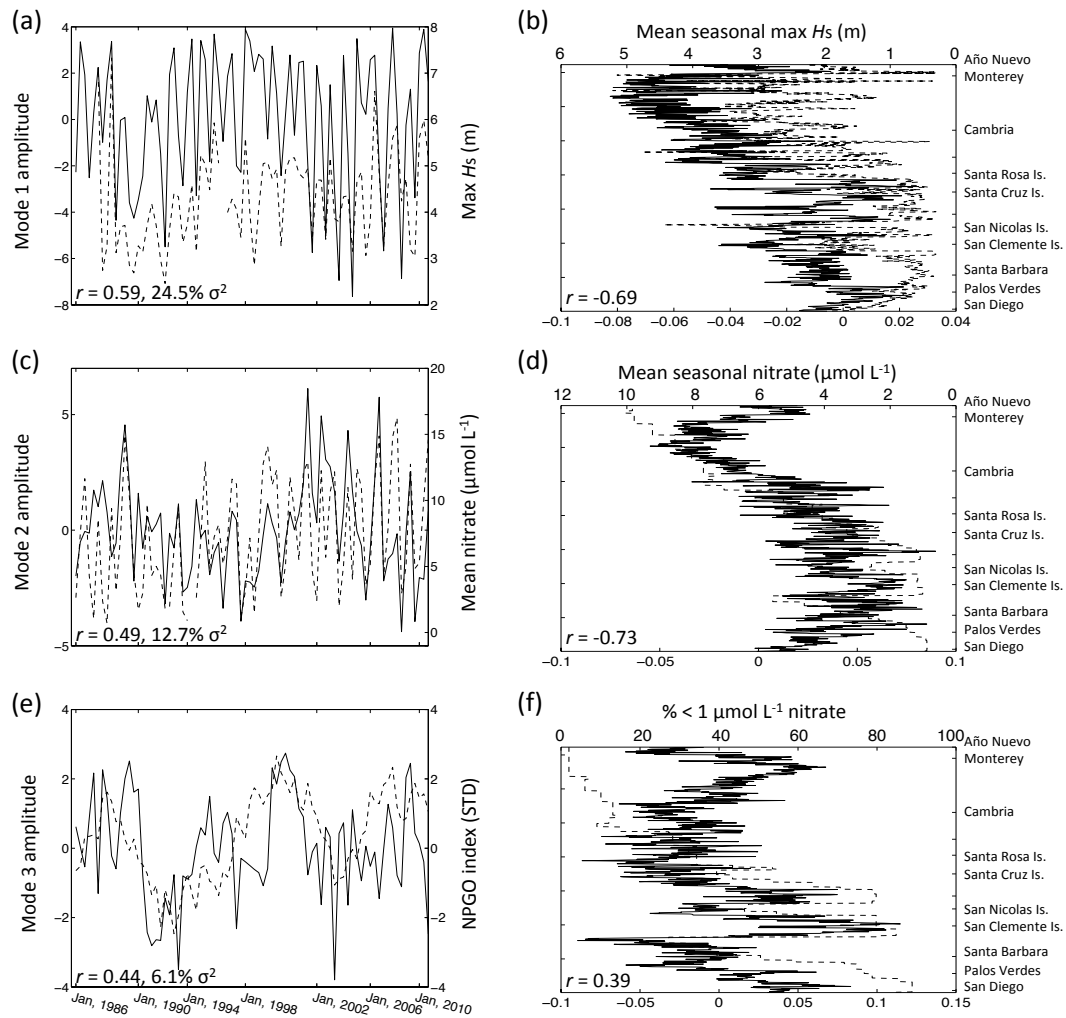
Figure 2.3. (a) Variance of giant kelp canopy biomass explained by a generalized additive model at each site, along the coast of California, USA. Vertical line is the ensemble mean R^2. (b–g) z-score standardized coefficient of each significant ($\alpha = 0.05$) predictor (maximum significant wave height (H_s), mean nitrate, North Pacific Gyre Oscillation index (NPGO), kelp occupancy, harvest effort, and sea urchin density) at each site. Mean nitrate concentrations estimated from sea-surface temperature. Sea urchin density observations were available from 45 of the 723 sites. Areas inside dashed lines represent the offshore Channel Islands.
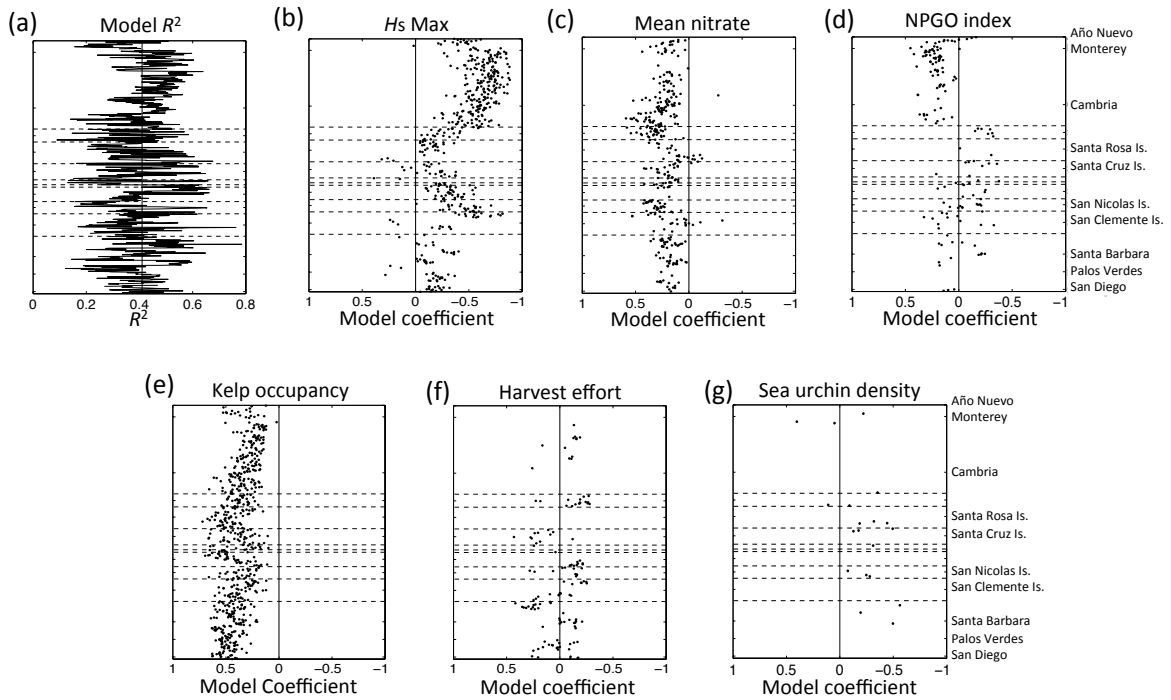
Figure 2.4. Additive effect of each environmental predictor variable on the site-specific generalized additive giant kelp canopy biomass model over the measured range of each predictor along the coast of California, USA (maximum significant wave height (H_s), mean nitrate, North Pacific Gyre Oscillation index (NPGO), kelp occupancy, harvest effort, and sea urchin density). The solid line is the mean effect of the predictor and the shaded regions show the 95% confidence intervals across all sites were the predictor was significant at α = 0.05. The frequency of each variable through space and time is shown by the histogram at the bottom of each effect plot. Mean nitrate concentrations estimated from sea-surface temperature. Sea urchin density observations were available from 45 of the 723 sites.
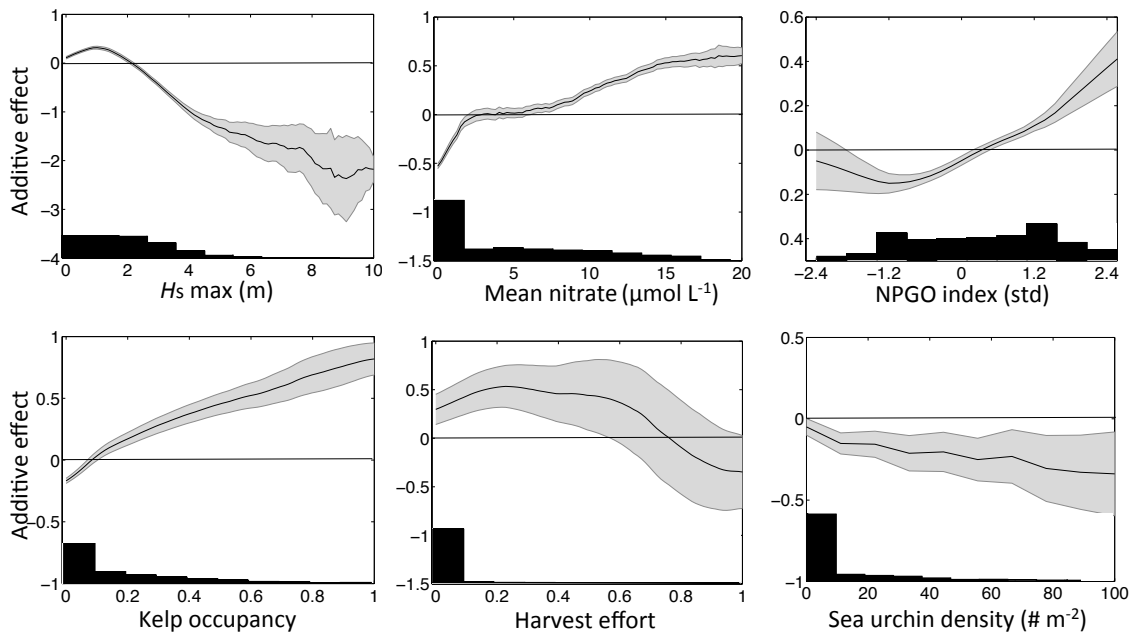
Figure 2.5. Giant kelp canopy biomass (solid line) at the Carpinteria kelp forest site, near Santa Barbara, California, compared with the model predictions (dashed line) based on relationships with wave disturbance, nitrate concentrations, North Pacific Gyre Oscillation index, and kelp occupancy. Annual sea urchin density is shown as black dots.
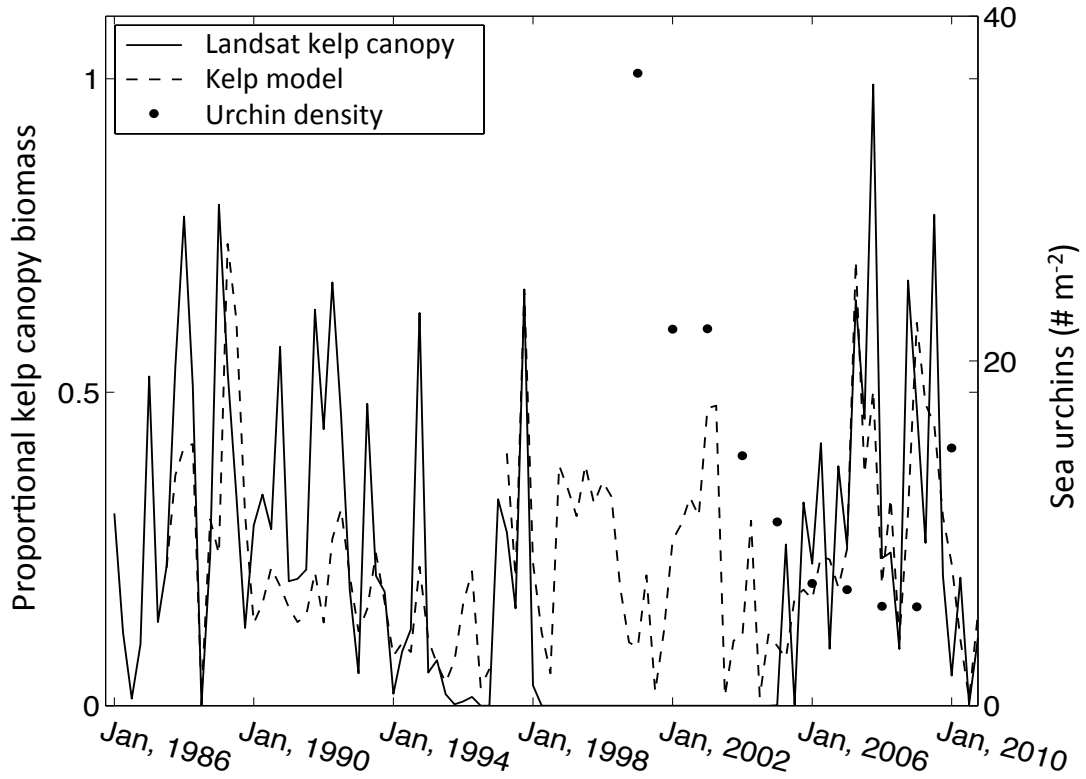
III. Giant kelp biomass and net primary productivity dynamics are associated with regional patterns of physiological condition

Abstract

Marine autotrophs vary their photosynthetic pigments in relation to their carbon mass (Chl:C) in response to changing environmental conditions. The Chl:C has been used as a proxy for the physiological condition of phytoplankton, and there is laboratory evidence that the growth rate of giant kelp (*Macrocystis pyrifera*) is strongly related to its Chl:C in nutrient-limited conditions. Understanding the relationship between Chl:C and net primary production of this species is important as it provides a key source of energy and structure for an economically significant and ecologically diverse ecosystem. We found that photosynthetic pigment state and Chl:C of the kelp canopy more closely resembles changes in available nitrate rather than changes in available light at locations in the Southern California Bight, while the reverse is true along the more nutrient-replete central California coastline. Photosynthetically available radiation and nitrate concentration acted antagonistically to explain 70% of the variation in Chl:C of the kelp canopy. Chl:C was positively related to changes in kelp biomass integrated over a three-month time scale at the periodically nutrient-limited southern California sites. Time series of net primary production estimated through correlations with kelp canopy biomass and lagged Chl:C compared well to estimates from more complex methods. These results open the possibility of estimating net primary production of giant kelp over large spatial and temporal scales using present and planned remote sensing technologies and the modeling of Chl:C based on well measured environmental variables.

A. Introduction

The physiological condition of marine flora fluctuates through time and space in response to environmental variability. As light, nutrient, and temperature conditions change, marine autotrophs vary cellular pigment levels to adjust to new photosynthetic demands (Kirk 1994). In a steady-state, nutrient-limited culture, the marine diatom, *Thalassiosira fluviatilis*, now *T. weissflogii*, was shown to linearly increase its cellular concentrations of chlorophyll *a* (Chl*a*), in relation to its carbon content (Chl:C; a known proxy for physiological condition) as nutrient limitations were released (Laws and Bannister 1980). The same diatom under nutrient-replete conditions decreased its Chl:C in a non-linear fashion in response to the addition of light. These results illustrate the potential of using measurements of Chl:C to diagnose physiological limitations in phytoplankton populations.

Environmentally forced fluctuations in photosynthetic pigments are not limited to phytoplankton but apply to marine photoautotrophs in general. For example, four species of seagrasses were also found to non-linearly increase Chl*a* concentrations in response to decreases in available light, in experiments simulating increased turbidity (Wiginton and McMillan 1979). Furthermore, seagrasses increased chlorophyll content and photosynthetic activity, and by extension growth rates and biomass accumulation in response to fertilizer additions while in a nutrient-limited environment (Agawin et al. 1996). These physiological responses appear to be similar across temperate and tropical seagrass species; a testament to the generality of extrinsic environmental factors affecting physiological condition dynamics in marine plants (reviewed in Leoni et al. 2008).

Values of the Chl:C ratio also scale with growth rate in phytoplankton and marine plants (e.g., Geider 1987; Shivji 1984). Sakshaug and others (1989) found that, in a nutrient-

limited system, the Chl:C ratio was linearly proportional to the growth rate of a marine

diatom for a given level of daily irradiance. Over the past decade, results from these and

other laboratory studies have been combined with large spatial scale measurements of Chl *a*

concentrations, phytoplankton carbon biomass, and incident light from satellite sensors to

estimate phytoplankton growth rates for the global oceans (Behrenfeld et al. 2005).

Phytoplankton and plant growth rates combined with carbon biomass determinations can

then be used to estimate regional net primary production, the basis for ecosystem production

and biogeochemical cycling (Jansen et al. 2015; Maiti et al. 2016; Wheeler et al. *in review*).

This example shows how the knowledge of an organism's physiological condition can

improve our ability to estimate the production dynamics of important primary producers.

The marine macroalga *Macrocystis pyrifera*, hereafter referred to as giant kelp, is a

globally distributed canopy forming species that serves as the foundation to an ecologically

diverse and economically important ecosystem (Leet et al. 2001; Graham et al. 2007; Schiel

& Foster 2015). This species is microscopic when it attaches to shallow (<30m depth) rocky

reefs, but can reach the surface and form a dense canopy within several months (Dayton et

al. 1992; Reed et al. 2006). The adult plant consists of a holdfast supporting a bundle of

fronds with leaf-like blades extending off at regular intervals, each with a gas-filled

pneumatocyst to buoy the fronds to the surface. The fronds commonly grow about 14 - 18

cm a day, which requires high concentrations of nutrients from the surrounding waters

(Gerard 1982; Zimmerman and Kremer 1986; Stewart et al. 2009). Frond elongation rate

increases in a non-linear, saturating fashion in response to increased ambient nitrate

concentrations (Zimmerman and Kremer 1984). Photosynthetic pigment concentrations and

Chl:C are also known to increase with elevated ambient nitrate conditions and be positively

39

associated with increases in specific growth rate under nutrient-limited conditions (Shivji 1984; Shivji 1985; Kopczak 1994).

Photosynthetic pigments and rates vary in giant kelp in response to changes in light along a depth gradient. Pigment content increases to a maximum in the canopy about 2 m back from the apical meristem and remains generally constant throughout much of the water column, until decreasing again in the oldest, deepest blades (Wheeler 1980, Rodriguez et al. 2016). The variation in pigment was found to be dynamic as it changed within days of juvenile sporophytes being transplanted from depth to the surface (Wheeler 1980). Despite these changes in pigment, photosynthetic rates remained constant, a pattern expected due to changes in irradiance when nutrients are not limiting. Surface canopy blades have higher ultraviolet absorbing compounds and photoprotective pigment concentrations than blades at depth, allowing canopy blades to present the highest relative photosynthetic rates and make the largest contribution to production (Colombo-Pallotta et al. 2006).

While much is known about how giant kelp responds to changes in light over a depth gradient at a single point in time, there is a dearth of research observing changes in physiological condition through time and over a latitudinal gradient. Understanding the relationships between the environment and growth of this foundational species would allow for the estimation of a major source of production entering this diverse and important food web. In this study, we aimed to determine the environmental drivers of giant kelp photosynthetic pigment concentration and Chl:C over multiple years at sites spanning ~750 km of coastline in California, USA. We related measurements of Chl:C to field and remotely sensed time series of kelp biomass and net primary production to expose nonlinear and time integrated relationships. Due to the expectation that light and nutrients should act

antagonistically to balance photosynthetic pigments and Chl:C, and that changes in the Chl:C are expected to modulate growth rate in nutrient-limited systems, we aimed to answer two overarching questions: (1) What are the relative roles of nutrients and light to the photosynthetic pigment and Chl:C dynamics of the giant kelp canopy? (2) Are these fluctuations in physiological condition related to changes in giant kelp biomass and net primary production over ecologically relevant time scales?

B. Methods

1. Giant kelp condition, biomass, and net primary production data

We assessed the physiological condition and biomass of the giant kelp canopy across the species' range of dominance in California, USA. This region is subject to seasonal fluctuations in both the surface nutrient and light environment. Sea surface nitrate concentrations follow seasonal and geographic patterns consistent with coastal upwelling in the California Current with northern areas along the central coast typically experiencing cooler, nutrient-rich water for longer periods of the year (Bernal and McGowan 1981; Bograd et al. 2001; Bograd et al. 2009). Kelp forests south of Point Conception, in southern California, are subject to lower nutrient conditions, with summer and fall nitrate concentrations falling below 1 μmol L^{-1}, the concentration were frond elongation rate begins to decline (Zimmerman & Kremer 1984; Reed et al. 2011). We sampled five kelp forest sites within this range: Pleasure Point (36.9564 N, 121.9641 W) near Santa Cruz, Arroyo Quemado (34.4677 N, 120.1191 W), Arroyo Burro (34.4003 N, 119.7446 W), and Mohawk (34.3941 N, 119.7296 W) in the Santa Barbara Channel, and La Jolla (32.8532 N, 117.2750W) near San Diego. Sites in the Santa Barbara Channel were sampled monthly by

41

the Santa Barbara Coastal Long Term Ecological Research (SBC LTER) project (August 2012 – August 2015), while sites in Santa Cruz and San Diego were sampled quarterly (June 2013 – July 2015). At each sample date, 15 mature canopy blades were haphazardly collected from different individuals. To standardize age, all blades were collected two meters from the tip of an actively growing frond. Blades were placed in a resealable plastic bag, which was then stored on ice in an opaque cooler for transport to the laboratory. Blades were then stored at 4°C until processed, which occurred within 24 hours of collection.

Once at the laboratory, a 5 cm^2 disc was excised from the central portion of each blade, cleaned of epiphytes and rinsed in a 10% HCl solution. The 15 discs for each site were combined and weighed to record wet mass, then dried at 60°C for several days, after which, dry mass was recorded. The pooled discs were then ground to a fine powder using a mortar and pestle and analyzed for carbon and nitrogen content using an elemental analyzer (Carlo-Erba Flash EA 1112 series, Thermo-Finnigan Italia, Milano, Italy). A separate 0.8 cm^2 disc was excised adjacent to the larger disc for pigment analysis. Each disc was blotted dry and weighed, then placed in 4mL dimethyl sulfoxide for 45 minutes at room temperature in the dark. The disc was then removed and washed with 1 mL water, which was added to the dimethyl sulfoxide extraction, and then placed in 5 mL of a mixture of 3:1:1 acetone, methanol, and water for 2 hours at 4°C in the dark. Upon removal from the second extract the disc was a pale white color, indicating no remaining pigment (Wheeler 1980). The separate extracts were then placed in individual quartz cuvettes and absorbance was measured from 350 – 800 nm using a spectrophotometer (Shimadzu UV 2401PC, Tokyo, Japan). Concentrations of chlorophyll *a* (Chl *a*), chlorophyll *c* (Chl *c*), and fucoxanthin (FX) were calculated from absorbance at several wavelengths allowing for determination by

empirical equations following Seely et al. 1972. Chl:C was calculated by dividing the molar mass of Chl *a* by the dry mass of carbon for each disc.

Standing foliar biomass and net primary production were estimated monthly for the three Santa Barbara Channel sites by the SBC LTER (Rassweiler et al. 2013). Briefly, divers estimate standing foliar biomass, defined as the total plant biomass excluding the holdfast and reproductive sporophylls, and the proportion of giant kelp fronds and plants removed by senescence or disturbance processes in permanent plots monthly (200 m^2 for Arroyo Quemado and Mohawk; 480m^2 for Arroyo Burro). Each month divers characterized the length of each plant (> 1m in height) in three distinct plant sections: the subsurface (fronds which do not reach the surface), the water-column (the subsurface portion of canopy fronds), and the canopy (the surface portion of canopy fronds). Divers also count the number of fronds at 1 m above the bottom and at the surface. From these measurements, standing foliar biomass is estimated based on empirical relationships between these allometric measurements and total plant wet mass. Frond and plant loss rate is calculated by tagging the fronds of 10 – 15 haphazardly selected plants in each plot, and recording the loss of tagged fronds and plants at each time point. Net primary production is then calculated as the total amount of biomass produced during the period between each sampling date that explains the observed changes in standing foliar biomass given the frond and plant loss rate for that period. Detailed methods are presented in Rassweiler et al. 2008. To account for noise between months, a three-month running mean was applied to the monthly net primary production data.

In order to generate consistent time series of giant kelp canopy fluctuations across all sites, including those not sampled by the SBC LTER, canopy biomass was estimated using the Landsat 7 Enhanced Thematic Mapper Plus and Landsat 8 Operational Land Imager satellites (detailed methods in Cavanaugh et al. 2011; Cavanaugh et al. 2014; Bell et al. *in prep*). The combination of these two sensors provides an image of the study area every eight days, and a cloud-free image approximately once a month. Briefly, images are atmospherically corrected and radiometrically standardized using 50 temporally stable pseudo-invariant targets (85 targets for Landsat 7 images to account for missing data due to the scan line corrector error; Furby & Campbell 2001). Multiple endmember spectral mixing analysis was then used to model each 30 x 30 m pixel as a linear combination of 2 endmembers; one temporally and spatially stable kelp endmember and one of 30 seawater endmembers unique to each image (Roberts et al. 1998). Multiple seawater endmembers were chosen to account for spatial and temporal differences in water conditions due to sediment, glint, phytoplankton, etc. Kelp canopy biomass was then estimated using an empirical relationship between diver estimated kelp canopy biomass and fractional kelp cover in each pixel. A long-term (2002 – 2015) comparison of Landsat kelp fraction with diver estimated kelp biomass in the Santa Barbara Channel explains 62.4% of canopy biomass dynamics (Cavanaugh et al. 2011; Bell et al. *in prep*). A monthly time series of kelp canopy biomass was generated for each site over the study period by summing all Landsat pixels within a 100m radius of each sampling site.

2. Environmental datasets

Spatio-temporal datasets of environmental variables known to be associated with fluctuations in the physiological condition of marine autotrophs were compiled from measured and remotely sensed sources. In the California Current, as with other coastal upwelling systems, a non-linear inverse relationship exists between temperature and nutrients, allowing for the estimation of surface nitrate concentration from more spatially and temporally explicit measurements of sea surface temperature (Zimmerman & Kremer 1984; Palacios et al. 2013). We developed a non-linear fit between measured surface temperature and nitrate concentrations from 26 years (1990 – 2015) of California Cooperative Oceanic Fisheries Investigations (CalCOFI) oceanographic cruises spanning the latitudes of our study sites (calcofi.org). We then produced a time series of surface nitrate concentrations at each of the five study sites using the nearest 9 km pixel of daily sea surface temperature from the MODIS Aqua satellite sensor (oceandata.sci.gsfc.nasa.gov). Daily determinations of photosynthetically active radiation (PAR) at the sea surface at 9 km spatial resolution was obtained from the MODIS Aqua satellite sensor (oceandata.sci.gsfc.nasa.gov).

3. Relationship of environment to kelp pigment and physiological condition dynamics

In order to assess the effect of changes in available nutrients and light and kelp canopy physiological condition, we examined the relationship between known environmental driver data and the giant kelp canopy photosynthetic pigment concentrations and Chl:C. We would expect that the concentration of ambient nitrate and PAR affect the physiological condition of giant kelp across different time scales. We constrained these time

effects by modeling photosynthetic pigments, carbon content, and Chl:C from all sites as a function of mean nitrate concentration and mean PAR over various time lags. As there was unequal sampling effort across sites, we randomly resampled the data so that all sites had the same number of measurements.

Once the appropriate time lag was found for each predictor variable, we used generalized least squares regressions to model each response variable as a function of nitrate and PAR for each region (nlme package; Pinheiro et al. 2016; R Core Team 2016). Generalized least squares regressions were used to account for autocorrelation between the residuals of the model. Beta, or standardized, coefficients were then calculated using the std_beta function (sjmisc package; Lüdecke 2016). To investigate the non-linearity of the effects of nitrate concentrations and PAR on the physiological condition of the giant kelp canopy, we used a generalized additive model with a Gaussian error distribution and the identity link function (mgcv package; Wood 2006). This approach models the response variable as the sum of non-linear functions of several predictor variables. Smoothness parameters were estimated with generalized cross validation. Data were resampled to account for differences in sampling effort across sites and the final model was validated using 5-fold cross validation.

4. Relationship of physiological condition to the dynamics of canopy biomass and net primary production

Giant kelp biomass has been shown to be a function of the quantity of biomass present in the preceding season (Reed et al. 2008; Bell et al. 2015a). To account for these dynamic starting conditions, changes in giant kelp canopy biomass through time were

assessed by examining the residuals of an autoregressive time series model. At each site, we linearly regressed Landsat estimated canopy biomass at time t by canopy biomass at time $t - 3\ months$. We then examined the residuals, which represent the change in kelp biomass over the season with respect to the starting conditions, and compared these to our time series of site-specific physiological condition using simple linear correlations.

Monthly net primary production was modeled at the three sites in the Santa Barbara Channel as a function of diver estimated standing foliar biomass and measured Chl:C over multiple time lags using generalized additive models (mgcv package; Wood 2006). The potentially non-linear relationships between the predictor variables and net primary production were examined and model selection was based on the generalized cross validation score. Models were constructed using a Tweedie error structure (power function = 1.1) with a log link and an AR(1) autoregressive model to account for temporal autocorrelation among residuals (mgcv package; Wood 2006). The Tweedie family error structure allows for a variable variance power function to fit the error structure of the data. Net primary production was then predicted based on the results of the generalized additive model and compared to the SBC LTER net primary production model for each site using simple linear correlations.

C. Results

1. Spatio-temporal variability in photosynthetic pigments and physiological condition

The Santa Cruz site experienced consistently higher nitrate concentrations in the surface waters throughout the year when compared to the southern California sites (Figure

1a). The Santa Barbara Channel sites experienced periodic increases in nitrate

concentrations in the surface waters associated with spring upwelling and low (<1 μmol L^{-1})

concentrations during the summer and fall. The San Diego site was characterized by low

nitrate concentrations in the surface waters throughout the measurement record. PAR values

followed a predicable seasonal cycle at all sites with slight variation between sites due to

latitude, clouds, and sampling dates (Figure 1b). Chl*a* and FX pigment concentrations as

well as Chl:C, followed a cyclical pattern that varied slightly by region (Figure 1c-e).

Carbon content displayed a more erratic pattern though time (Figure 1f). The photosynthetic

pigments displayed larger variations than carbon content when compared to their means,

with coefficients of variation of 0.43 for Chl*a*, 0.38 for FX, and 0.22 for carbon content.

Time lags were consistent for the photosynthetic pigments Chl*a*, FX, and FX:Chl*a*,

with a optimal lag of 5 days for nitrate and 18 days for PAR. Chl:C maintained an 18 day

lag for PAR, but increased the lag to 11 days for nitrate concentration. All environmental

variables were significant at the $p = 0.05$ level for the optimal lag times. Carbon content

showed a nitrate lag of 19 days and a PAR lag of 18 days, although neither predictor was

significant at the $p = 0.05$ level.

Concentrations of photosynthetic pigments at the Santa Cruz site were all negatively

associated with changes in amount of PAR and not significantly related to changes in

surface water nitrate concentrations (Table 1). In contrast, pigment concentrations at sites in

the Santa Barbara Channel were positively related to changes in nitrate concentration. Chl*a*

and FX concentrations were negatively related to changes in PAR at the Santa Barbara

Channel sites, however beta coefficient analysis showed that nitrate concentration effect was

about 3x that of PAR. Changes in pigment concentrations at the San Diego site were not found to be significantly related to nitrate concentrations or PAR. The ratio of fucoxanthin pigment to chlorophyll a pigment (FX:Chl*a*) was positively related PAR at the Santa Cruz site, and was positively related to PAR and negatively related to nitrate concentrations at the Santa Barbara Channel sites. Carbon content was not significantly related to changes in nitrate concentrations or PAR at any site. Chl:C was negatively related to PAR at the Santa Cruz site, positively related to nitrate concentrations at the San Diego site, and both negatively related to PAR and positively related to nitrate concentrations at the Santa Barbara Channel sites.

The Chl:C of the surface canopy was modeled as non-linear functions of both surface water nitrate concentrations and PAR. Both variables were found to be significantly related to changes in Chl:C (R^2 = 0.70, p < 0.001). Chl:C was negatively related to nitrate at low concentrations (0 to 0.5 μmol L^{-1}), but showed an increasingly positive relationship up to ~2 μmol L^{-1} (Figure 2a). There was no increasing effect of nitrate concentration on Chl:C from 2 to 4 μmol L^{-1}, this was followed by a weak increasing trend for nitrate concentrations above ~4 μmol L^{-1}. PAR had a positive effect on Chl:C from 15 to ~30 Einsteins m^{-2} d^{-1} and a little effect as values increased from ~30 to 60 Einsteins m^{-2} d^{-1} (Figure 2b).

2. Relationship between canopy biomass dynamics and physiological condition

At the northern Santa Cruz site, canopy biomass tended to be highest during the summer and lower during the winter months (Figure 3a). At the southern California sites, canopy biomass increased throughout 2013 and began to decline throughout 2014. Most canopy was lost during 2015 with few increases (Figure 3b-e). The dependence on the Chl:C

on the standing biomass in previous months varied greatly between central and southern California. Canopy biomass at a given time point was significantly related to canopy biomass three months in the past at all three Santa Barbara Channel sites: Arroyo Quemado ($r^2 = 0.20$, $p < 0.01$, n = 34), Arroyo Burro ($r^2 = 0.27$, $p < 0.01$, n = 19), Mohawk ($r^2 = 0.23$, $p < 0.01$, n = 34). Temporal autocorrelation was marginally significant at the San Diego site ($r^2 = 0.25$, $p = 0.10$, n = 9) and was non-significant at the Santa Cruz site ($r^2 = 0.05$, $p = 0.48$, n = 9). The biomass residuals of these autocorrelation functions were not significantly related to the sampled Chl:C time series at the Santa Cruz site (Figure 3a). However Chl:C was significantly and positively related to residuals from the three Santa Barbara Channel sites with a temporal lag time of two months (Figure 3b-d). Residuals from the Arroyo Burro site were not available after April 2014 as canopy biomass was too low to be detected by the Landsat sensor. The residuals from the San Diego site were also significantly related to Chl:C with a temporal lag time of three months (Figure 3e).

3. Relationship between net primary production and physiological condition

Predictions of net primary production based on the generalized additive model that accounted for standing biomass and Chl:C closely matched those of the SBC LTER model at all three sites (Arroyo Quemado: r = 0.954, $p < 0.001$; Arroyo Burro: r = 0.813, $p < 0.001$; Mohawk: r = 0.784, $p < 0.001$; Figure 4). The relationship between standing foliar biomass and net primary production was asymptotic ($p < 0.001$; Figure 5a). There was a linear increase in the additive effect on net primary production as standing foliar biomass increased from $0 - 3$ kg m^{-2}, becoming positive at 2 kg m^{-2}, reaching an asymptote from $3 - 9$ kg m^{-2}. Chl:C was significantly related to net primary production with a temporal lag of 6 months (p

< 0.001). There was near linear increase in the additive effect of the Chl:C state of the canopy to net primary production with a 6-month time lag, with positive effects occurring at Chl:C greater than 0.0125 mg mg^{-1} (Figure 5b). Using Chl:C and standing foliar biomass as predictors improved the model fit from $R^2 = 0.65$ to 0.74, and reduced the generalized cross validation score from 0.00223 to 0.00196 versus using standing foliar biomass as the sole predictor variable.

D. Discussion

1. Spatial heterogeneity in drivers of photosynthetic pigment state and physiological condition

Understanding the effect of physiological condition on the dynamics of giant kelp is challenging as the variability of this foundational species is controlled by a combination of top-down, bottom-up, and disturbance forces (Schiel & Foster 2015). One way to begin to tease apart these environmental effects on physiological condition is to examine changes in photosynthetic pigments and other physiological proxies over a spatial gradient of environmental conditions. The range of giant kelp in the NE Pacific spans a variety of light and nutrient environments, from the large seasonal light fluctuations of SE Alaska to the often warm, nutrient-poor waters of southern and Baja California (Graham et al. 2007). Therefore, we should expect this species to adjust its photosynthetic pigment concentrations according to its local environmental conditions.

During nutrient-replete conditions, marine autotrophs tend to increase pigment concentrations during low light seasons and decrease pigment concentrations during periods

of high light (Wiginton and McMillan 1979). It is not surprising then that fluctuations in photosynthetic pigments at Santa Cruz were strongly and negatively associated with changes in PAR rather than nutrients because kelp at this site is bathed in cool, nutrient-rich water throughout most of the year. Kelp canopy pigments in the Santa Barbara Channel showed a different pattern than the northern Santa Cruz site, as relatively high pigment levels were sometimes observed during periods of high light availability. Pigment concentration patterns closely mirrored seasonal and interannual variation in nitrate concentrations in the more oligotrophic waters of the Santa Barbara Channel. The light modulated relationship of the ratio of the accessory photosynthetic pigment FX to Chl*a* may highlight an additional photoprotective function. While other accessory pigments ratios have shown a negative relationship to light levels, FX is an exception to this rule in other brown algae and diatom species (Brown & Richardson 1968). Carotenoid pigments like FX are light-harvesting pigments, however they can also exert a protective effect against photooxidation of cell material in high light environments, so this positive association with PAR levels may be an adaptive response (Clayton 1980; Di Valentin et al. 2012).

The patterns in Chl:C, our proxy for physiological condition, were also tied to fluctuations in light and nutrient conditions across the three regions. Seawater nitrate concentration has an increasingly positive relationship with physiological condition as one moves from the northern to southern sites where nutrient limitation should be more prevalent (Table 1). The differences in the magnitude of the relationships of nitrate concentration and PAR to the Chl:C of the kelp canopy are the result of nonlinear effects. The nonlinear relationship with nitrate showed a linear increase at concentrations from $0 - 2$ μmol L^{-1} (Figure 2a). This pattern fits with other studies that showed the growth of juvenile

kelp plants increased sharply over this range, and the observed reduction in frond elongation rate at nitrate concentrations < 1 μmol L^{-1} (Kopczak et al 1991; Gerard 1982; Zimmerman & Kremer 1984; 1986; Brzezinski et al. 2013). The steep decline in effect size for all but the lowest observed PAR values suggests that light limitation has little effect on the Chl:C of the giant kelp canopy in much of California except during the winter months (Figure 2b).

2. The role of physiological condition in giant kelp dynamics

The present state of a system is often a good predictor of that system's state in the near future. This statement can be extended to giant kelp forests where the amount of canopy biomass at present often foretells the biomass in the following season (Bell et al. 2015a). Temporal autocorrelation explained a greater proportion of kelp forest biomass dynamics in southern California compared to central California, likely because seasonal cycles are more pronounced in the north due to greater wave disturbance in winter (Reed et al. 2011; Bell et al. 2015a; 2015b). Consequently canopy biomass was not positively related to Chl:C at Santa Cruz which tended to show high pigment levels in the winter when canopy biomass was typically at its lowest point. Photosynthetic pigments and physiological condition were also strongly correlated with PAR at Santa Cruz suggesting that the kelp canopy can freely adjust pigment concentrations in response to changing light conditions because nutrient concentrations are typically high (Table 1).

The positive relationship between changes in canopy biomass and Chl:C suggests that the physiological state of the canopy plays a role in the biomass dynamics of the often nutrient-limited southern California kelp forests (Figure 3b-e). These changes in canopy biomass involve several processes integrated over different time scales. For instance,

53

increases in frond elongation rates, which are related to the external nutrient environment, will manifest as canopy biomass accumulation over time as fronds grow and reach the surface or add to their surface length (Zimmerman & Kremer 1986). Additionally, frond dynamics are dominantly controlled by programmed senescence in which an individual frond has an average lifespan of ~100 days (Rodriguez et al. 2013). Fluctuations in canopy biomass may persist on timescales longer than the environmental changes which driven them.

Increases in biomass over a given period of time represent net primary production, which is the portion fixed carbon that remains after plant respiration (Chapin et al. 2002). The most comprehensive time series of net primary production in giant kelp relies on *in situ* measurements of changes in standing biomass from one period to the next, while simultaneously constraining several processes of biomass loss (Rassweiler et al. 2008; Reed et al. 2015). Simplifying the estimation of net primary production to a function of the present biomass state and lagged Chl:C compared well with this previous method (Figure 4). This simplification removes the need to estimate losses and opens the possibility of net primary production estimates over large spatial scales with available (or soon to be available) remotely sensed products (discussed below). We found a positive relationship between foliar standing biomass and net primary production that saturated at ~ 6 kg m^2. One possible explanation for this relationship is a reduction in photosynthesis due to density dependent shelf shading as the size and biomass of the forest increases. Stewart and others (2009) found that canopy fronds growing on the offshore edge of the Mohawk kelp forest in the Santa Barbara Channel displayed a higher growth rate than canopy fronds growing in the

interior of the bed. Since giant kelp grows on limited areas of rocky reef, biomass may be added without any increase in edge area as the reef nears carrying capacity.

The physiological state of the canopy is implicitly associated with net primary production through the accumulation of biomass, however there was also a significant positive linear relationship with Chl:C with a 6 month lag (Figure 5b). This raises the possibility of longer-term associations in giant kelp robustness or demographics linked with physiological condition in the past. Stephens and Hepburn (2016) found that increases in seawater nitrate concentration increased photosynthetic pigment concentrations as well as the thickness of mature kelp blades, leading to enhanced tissue integrity and lower rates of blade erosion. This effect of environmental condition on the quality of kelp biomass, not merely the quantity, may lead to lagged effects on future growth potential through frond initiation dynamics, as frond elongation and initiation rates are positively related (Gerard 1976; Zimmerman 1983). There may also be an indirect link of environmental conditions associated with physiological condition and kelp demographics. Kelp spore quality and quantity is associated with resource availability, where cooler, nutrient-rich water leads to increases in spore standing stock and decreases in the carbon:nitrogen ratio, while also leading to greater sorus area during the first half of the year when upwelling conditions were strongest (Reed et al. 1996; Castorani et al. *in review*). Additionally, Deysher and Dean (1986) reported the existence of giant kelp recruitment windows, where there was increased recruitment at cooler seawater temperatures associated with higher nutrient concentrations. It would be months before the microscopic recruits reached the size threshold (> 1 m tall) to be included in our estimates of foliar standing biomass (Rassweiler et al. 2008). There was a significant positive response of specific growth rate with changes in the proportion of recruit

biomass to total biomass, suggesting that young plants grew faster than older plants (Reed et al. 2008). Periods of time with poor environmental conditions leading to a closure of the recruitment window might reduce future net primary production, as the age structure of the forest becomes skewed towards older plants.

3. Estimation of net primary production from remotely sensed imagery

Recent advances in the remote estimation of giant kelp biomass and physiological condition have revealed how its biomass dynamics are associated with changes in environmental conditions (Cavanaugh et al. 2011; Bell et al. 2015a; 2015b; Young et al. 2016). Results presented here show how information on kelp biomass and the recent history of its physiological condition can be used to estimate net primary production. Currently, Landsat multispectral imagery is used to estimate canopy biomass of giant kelp forests in the NE Pacific (Cavanaugh et al. 2011; Bell et al. *in prep*). The inclusion of physiological condition in this estimation is important, as hyperspectral imagery has shown up to 2-fold differences in Chl:C across a single kelp forest when moving from the inshore to offshore edge (Bell et al. 2015b). The planned Hyperspectral Infrared Imager (HyspIRI) mission could provide global, repeat hyperspectral imagery on the appropriate spatial scales for estimating both giant kelp canopy biomass and physiological condition simultaneously (Lee et al. 2015; Hochberg et al. 2015; Bell et al. 2015b).

We have shown that the physiological condition of giant kelp canopy blades is a predictable function of sea surface nitrate concentrations and PAR (Figure 2), and both variables can be estimated from satellite imagery. Subregional (~4km resolution) data of estimated PAR and nitrate concentrations at the sea surface can be used with Landsat

estimates of kelp canopy biomass to generate estimates of net primary production. This potential time series could serve as a measure of carbon entering the giant kelp forest ecosystem through the giant kelp canopy, informing many active areas of research including food web dynamics, carbon storage, and changes associated with climate (Byrnes et al. 2011; Johnson et al. 2011; Wilmers et al. 2012; Koenigs et al. 2015; Morton et al. 2016; Reed et al. *in review*).

Fluctuations in environmental conditions are associated with changes in the photosynthetic pigment state and physiological condition of giant kelp canopy, however the strength of these associations varies regionally. Many of these processes linking physiological condition to biomass accumulation, and thus net primary production, are integrated over varied timescales, and translate to measureable changes over the course of several months. By leveraging the present state of kelp forest biomass, along with knowledge of the physiological state of the canopy or the environmental processes associated with it, and remote sensing tools, it may be possible to generate spatially expansive time series of net primary production for this important foundation species.

E. Chapter Acknowledgements

F. Literature Cited

Agawin, N., C. M. Duarte, and M. Fortes. 1996. Nutrient limitation of Philippine seagrasses (Cape Bolinao, NW Philippines): in situ experimental evidence. Mar. Ecol. Prog. Ser. **138**: 233–243.

Behrenfeld, M. J., E. Boss, D. A. Siegel, and D. M. Shea. 2005. Carbon-based ocean productivity and phytoplankton physiology from space. Global Biogeochem. Cycles **19**: 1–14. doi:10.1029/2004GB002299

Bell, T.W., J. Allen, K. C. Cavanaugh, and D.A. Siegel. *in prep*. Multidecadal views of giant kelp forests off California from the Landsat satellites.

Bell, T. W., K. C. Cavanaugh, D. C. Reed, and D. A. Siegel. 2015a. Geographical variability in the controls of giant kelp biomass dynamics. J. Biogeogr. **42**: 2010–2021. doi:10.1111/jbi.12550

Bell, T. W., K. C. Cavanaugh, and D. A. Siegel. 2015b. Remote monitoring of giant kelp biomass and physiological condition: An evaluation of the potential for the Hyperspectral Infrared Imager (HyspIRI) mission. Remote Sens. Environ. **167**: 218–228. doi:10.1016/j.rse.2015.05.003

Bernal, P., and J. A. McGowan. 1981. Advection and Upwelling in the California Current, F. Richards [ed.]. American Geophysical Union.

Bograd, S. J., T. K. Chereskin, and D. Roemmich . 2001. Transport of mass, heat, salt, and nutrients in the southern California Current System: Annual cycle and interannual variability. Journal of Geophysical Research-Oceans. **106**: 9255-9275.

Bograd, S. J., I. Schroeder, N. Sarkar, X. Qiu, W. J. Sydeman, and F. B. Schwing. 2009. Phenology of coastal upwelling in the California Current. Geophys. Res. Lett. **36**: 1602. doi:10.1029/2008GL035933

Brown, T. E., and F. L. Richardson. 1968. The Effect of Growth Environment on the Physiology of Algae: Light Intensity. J. Phycol. **4**: 38–54.

Brzezinski, M., D. Reed, and S. Harrer. 2013. Multiple Sources and Forms of Nitrogen Sustain Year-Round Kelp Growth on the Inner Continental Shelf of the Santa Barbara Channel. Oceanography **26**: 114–123.

Byrnes, J., D. Reed, B. Cardinale, K. Cavanaugh, S. Holbrook, and R. Schmitt. 2011. Climate driven increases in storm frequency simplify kelp forest food webs. Glob. Chang. Biol. **17**: 2513–2524. doi:10.1111/j.1365-2486.2011.02409.x

Castorani, M. C. N., D. C. Reed, P. T. Raimondi, F. Alberto, T. W. Bell, K. C. Cavanaugh, D. A. Siegel, R. D. Simons. *in review*. Fluctuations in population fecundity drive demographic connectivity and structure metapopulation dynamics. Philos. Trans. R. Soc. London B.

Cavanaugh, K. C., D. A. Siegel, D. C. Reed, and T. W. Bell. 2014. SBC LTER: Time series of kelp biomass in the canopy from Landsat 5, 1984 -2011. Santa Barbara Coastal LTER. doi:10.6073/pasta/329658f19d5e61dda0be5ee883cd1c41

Cavanaugh, K., D. Siegel, D. Reed, and P. Dennison. 2011. Environmental controls of giant-kelp biomass in the Santa Barbara Channel, California. Mar. Ecol. Prog. Ser. **429**: 1–17. doi:10.3354/meps09141

Chapin, F. S., III, P. A. Matson, and H. Mooney. 2002. Principles of terrestrial ecosystem ecology. Springer-Verlag, New York, New York, USA.

Clayton, R. K. 1980. Photosynthesis: physical mechanisms and chemical patterns. Cambridge University Press. Cambridge, United Kingdom.

Colombo-Pallotta, M. F., E. García-Mendoza, and L. B. Ladah. 2006. Photosynthetic Performance, Light Absorption, and Pigment Composition of *Macrocystis pyrifera* (Laminariales, Phaeophyceae) Blades From Different Depths. J. Phycol. **42**: 1225–1234. doi:10.1111/j.1529-8817.2006.00287.x

Dayton, P. K., M. J. Tegner, P. E. Parnell, and P. B. Edwards. 1992. Temporal and Spatial Patterns of Disturbance and Recovery in a Kelp Forest Community. Ecol. Monogr. **62**: 421–445.

Deysher, L., and T. Dean. 1986. In situ recruitment of sporophytes of the giant kelp, *Macrocystis pyrifera* (L.) C. A. Agardh: effects of physical factors. J. Exp. Mar. Biol. **103**: 41–63.

Di Valentin, M., C. Büchel, G. M. Giacometti, and D. Carbonera. 2012. Chlorophyll triplet quenching by fucoxanthin in the fucoxanthin-chlorophyll protein from the diatom Cyclotella meneghiniana. Biochem. Biophys. Res. Commun. **427**: 637–41. doi:10.1016/j.bbrc.2012.09.113

Furby, S. L., and N. A. Campbell. 2001. Calibrating images from different dates to "like-value" digital counts. Remote Sens. Environ. **77**: 186–196. doi:10.1016/S0034-4257(01)00205-X

Geider, R. J. 1987. Light and temperature dependence of the carbon to chlorophyll *a* ratio in microalgae and cyanobacteria: implications for physiology and growth of phytoplankton. New Phytol. **106**: 1–34.

Gerard, V. A. 1976. Some aspects of material dynamics and energy flow in a kelp forest in Monterey Bay, California. Ph.D. dissertation, University of California, Santa Cruz, 173 pp.

Gerard, V. A. 1982. Growth and utilization of internal nitrogen reserves by the giant kelp *Macrocystis pyrifera* in a low-nitrogen environment. Mar. Biol. **66**: 27–35.

Graham, M. H., and A. H. Buschmann. 2007. Global ecology of the giant kelp *Macrocystis*: from ecotypes to ecosystems. Oceanogr. Mar. Biol. An Annu. Rev. **45**: 39–88.

Hochberg, E. J., D. A. Roberts, P. E. Dennison, and G. C. Hulley. 2015. Remote Sensing of Environment Special issue on the Hyperspectral Infrared Imager (HyspIRI): Emerging science in terrestrial and aquatic ecology, radiation balance and hazards. Remote Sens. Environ. **167**: 1–5. doi:10.1016/j.rse.2015.06.011

Jansen, T., P. Kainge, L. Singh, M. Wilhelm, D. Durholtz, T. Strømme, J. Kathena, and V. Erasmus. 2015. Spawning patterns of shallow-water hake (Merluccius capensis) and deep-water hake (M . paradoxus) in the Benguela Current Large Marine Ecosystem inferred from gonadosomatic indices. Fish. Res. **172**: 168–180. doi:10.1016/j.fishres.2015.07.009

Johnson, C. R., S. C. Banks, N. S. Barrett, and others. 2011. Journal of Experimental Marine Biology and Ecology Climate change cascades : Shifts in oceanography , species ' ranges and subtidal marine community dynamics in eastern Tasmania. J. Exp. Mar. Bio. Ecol. **400**: 17–32. doi:10.1016/j.jembe.2011.02.032

Kirk, J. T. O. 1994. Light and Photosynthesis in Aquatic Ecosystems. Cambridge University Press. Cambridge, United Kingdom.

Koenigs, C., R. J. Miller, and H. M. Page. 2015. Top predators rely on carbon derived from giant kelp *Macrocystis pyrifera*. Mar. Ecol. Prog. Ser. **537**: 1–8. doi:10.3354/meps11467

Kopczak, C. D. 1994. Variability of nitrate uptake capacity in *Macrocystis pyrifera* (Laminariales, Phaeophyta) with nitrate and light availability. J. Phycol. **30**: 573–580.

Kopczak, C. D., R. C. Zimmerman, and J. N. Kremer. 1991. Variation in Nitrogen Physiology and Growth Among Geographically Isolated Populations of the Giant Kelp, *Macrocystis pyrifera* (Phaeophyta). J. Phycol. **27**: 149–158.

Laws, E., and T. Bannister. 1980. Nutrient and light-limited growth of Thalassiosira fluviatilis in continuous culture, with implications for phytoplankton growth in the ocean. Limnol. Oceanogr. **25**: 457–473.

Lee, C. M., M. L. Cable, S. J. Hook, R. O. Green, S. L. Ustin, D. J. Mandl, and E. M. Middleton. 2015. An introduction to the NASA Hyperspectral InfraRed Imager (HyspIRI) mission and preparatory activities. Remote Sensing of Environment. **167**: 6-19.

Leet, W.S., Dewees, C.M., Klingbeil, R., & Johnson, E.J. 2001. California's living marine resources: A status report. State of CA Resources Agency and Fish and Game (593 pp.).

Leoni, V., A. Vela, V. Pasqualini, C. Pergent-Martini, and G. Pergent. 2008. Effects of experimental reduction of light and nutrient enrichments (N and P) on seagrasses: a review. Aquat. Conserv. Mar. Freshw. Ecosyst. **18**: 202–220. doi:10.1002/aqc

Lüdecke, D. 2016. sjmisc: Miscellaneous Data Management Tools. R package version 1.7.

Maiti, K., S. Bosu, E. J. D. Sa, P. L. Adhikari, M. Sutor, and K. Longnecker. 2016. Export fluxes in northern Gulf of Mexico - Comparative evaluation of direct, indirect and satellite-based estimates. Mar. Chem. in press. doi:10.1016/j.marchem.2016.06.001

Morton, D. N., T. W. Bell, and T. W. Anderson. 2016. Spatial synchrony of amphipods in giant kelp forests. Mar. Biol. 1–11. doi:10.1007/s00227-015-2807-5

Palacios, D. M., E. L. Hazen, I. D. Schroeder, and S. J. Bograd. 2013. Modeling the temperature-nitrate relationship in the coastal upwelling domain of the California Current. J. Geophys. Res. Ocean. **118**: 3223–3239. doi:10.1002/jgrc.20216

Pinheiro, J., D. Bates, S. DebRoy, D. Sarkar, and R Core Team. 2016. nlme: Linear and Nonlinear Mixed Effects Models. R package version 3.1-127.

Rassweiler, A., K. K. Arkema, and D. C. Reed. 2008. Net Primary Production, Growth, and Standing Crop of *Macrocystis pyrifera* in Southern California. Ecology **89**: 2068–2068.

Rassweiler, A. R., K. Arkema, D. C. Reed, R. C. Zimmerman, and M. A. Brzezinski. 2013. SBCLTER: Reef: Net primary production, growth and standing crop of *Macrocystis pyrifera* in Southern California. Santa Barbara Coastal LTER. doi:10.6073/pasta/b18fab7c03e0f4ab9bba716c7260a6ce

Reed, D. C., C. A. Carlson, E. R. Halewood, J. C. Nelson, S. L. Harrer, A. Rassweiler, and R. J. Miller. 2015. Patterns and controls of reef-scale production of dissolved organic carbon by giant kelp *Macrocystis pyrifera*. Limnol. Oceanogr. **60**: 1996–2008. doi:10.1002/lno.10154

Reed, D. C., A. Ebeling, T. W. Anderson, and M. Anghera. 1996. Differential Reproductive Responses to Fluctuating Resources in Two Seaweeds with Different Reproductive Strategies. Ecology **77**: 300–316.

Reed, D. C., B. P. Kinlan, P. T. Raimondi, L. Washburn, B. Gaylord, and P. T. Drake. 2006. A metapopulation perspective on patch dynamics and connectivity of giant kelp. Pages 352–386 in J. P. Kritzer and P. F. Sale, editors. Marine metapopulations. Academic Press, San Diego, California, USA.

Reed, D. C., A. Rassweiler, and K. K. Arkema. 2008. Biomass rather than growth rate determines variation in net primary production by giant kelp. Ecology **89**: 2493–2505. doi:10.1890/07-1106.1

Reed, D. C., A. Rassweiler, M. H. Carr, K. C. Cavanaugh, D. P. Malone, and D. A. Siegel. 2011. Wave disturbance overwhelms top-down and bottom-up control of primary production in California kelp forests. Ecology **92**: 2108–2116. doi:10.1890/11-0377.1

Reed, D. C., L. Washburn, A. Rassweiler, R. J. Miller, T. W. Bell. *in review*. Extreme warming challenges kelp forests as sentinels of climate change. Nature Communications.

Roberts, D. A., M. Gardner, R. Church, S. Ustin, G. Scheer, and R. O. Green. 1998. Mapping chaparral in the Santa Monica Mountains using multiple endmember spectral mixture models – II. Environmental influences on regional abundance. Remote Sensing of Environment, **65**: 267–279.

Rodriguez, G., A. Rassweiler, D. Reed, and S. Holbrook. 2013. The importance of progressive senescence in the biomass dynamics of giant kelp (*Macrocystis pyrifera*). Ecology **94**: 1848–1858.

Rodriguez, G.E., Reed, D.C. & Holbrook, S.J. 2016. Blade life span, structural investment, and nutrient allocation in giant kelp. Oecologia doi:10.1007/s00442-016-3674-6

Sakshaug, E., K. Andresen, and D. Kiefer. 1989. A steady state description of growth and light absorption in the marine planktonic diatom Skeletonema costatum. Limnol. Oceanogr. **34**: 198–205.

Seely, G., M. Duncan, and W. Vidaver. 1972. Preparative and analytical extraction of pigments from brown algae with dimethyl sulfoxide. Mar. Biol. **12**: 184–188.

Schiel, D. R. & Foster, M. S. 2015. The biology and ecology of giant kelp forests, University of California Press, Berkeley.

Shivji, M. S. 1984. Physiological responses of juvenile *Macrocystis pyrifera* sporophytes (Phaeophyta) to environmental factors: light, nitrogen and the interaction of light and nitrogen. M.A. Thesis in Biology, University of California, Santa Barbara, 51 pp.

Shivji, M. 1985. Interactive effects of light and nitrogen on growth and chemical composition of juvenile *Macrocystis pyrifera* (L.) C. At. (Phaeophyta) sporophytes. J. Exp. Mar. Bio. Ecol. **89**: 81–96.

Stephens, T. A., and C. D. Hepburn. 2016. A kelp with integrity: *Macrocystis pyrifera* prioritises tissue maintenance in response to nitrogen fertilisation. Oecologia **181**: 1–14. doi:10.1007/s00442-016-3641-2

Stewart, H., J. Fram, and D. Reed. 2009. Differences in growth, morphology and tissue carbon and nitrogen of *Macrocystis pyrifera* within and at the outer edge of a giant kelp forest in California, USA. Mar. Ecol. Prog. … **375**: 101–112. doi:10.3354/meps07752

Wheeler, S. G., T. W. Anderson, T. W. Bell, S. G. Morgan, J. A. Hobbs. *in review*. Regional productivity predicts individual growth and recruitment of rockfishes in a northern California upwelling system. Limnol. Oceanogr.

Wheeler, W. 1980. Pigment content and photosynthetic rate of the fronds of *Macrocystis pyrifera*. Mar. Biol. **56**: 97–102.

Wiginton, J. R., and C. Mcmillan. 1979. Chlorophyll composition under controlled light conditions as related to the distribution of seagrasses in Texas and the U.S. Virgin Islands. Aquat. Bot. **6**: 171–184.

Wilmers, C. C., J. A. Estes, M. Edwards, K. L. Laidre, and B. Konar. 2012. Do trophic cascades affect the storage and flux of atmospheric carbon? An analysis of sea otters and kelp forests. Front. Ecol. Environ. **10**: 409–415. doi:10.1890/110176

Wood, S.N. 2006. Generalized Additive Models: An Introduction with R. Chapman and Hall/CRC.

Young, M., K. C. Cavanaugh, T. W. Bell, P. Raimondi, C. A. Edwards, P. T. Drake, L. Erikson, and C. Storlazzi. 2016. Environmental controls on spatial patterns in the long-term persistence of giant kelp in central California. Ecol. Monogr. **86**: 45–60.

Zimmerman, R. C. 1983. Seasonal patterns in the productivity of a giant kelp (*Macrocystis pyrifera*) forest: the effect of nutrient availability. Ph.D. dissertation, University of Southern California, 182 pp.

Zimmerman, R. C., and J. N. Kremer. 1984. Episodic nutrient supply to a kelp forest ecosystem in Southern California. J. Mar. Res. **42**: 591–604. doi:10.1357/002224084788506031

Zimmerman, R. C., and J. N. Kremer. 1986. In situ growth and chemical composition of the giant kelp, *Macrocystis pyrifera*: response to temporal changes in ambient nutrient availability. Mar. Ecol. Prog. Ser. **27**: 277–285.

Table 3.1. Beta coefficients of the photosynthetic pigments chlorophyll *a* (Chl*a*) and fucoxanthin (FX) and pigment ratio (FX:Chl*a*), carbon content, and chlorophyll to carbon ratio (Chl:C) in relation to changes in nitrate concentration and photosynthetically available radiation at each site. Bold values are significant at $\alpha = 0.05$.

Site		Chl*a*	FX	FX:Chl*a*	Carbon	Chl:C
Santa Cruz	NO_3	-0.06	0.03	-0.49	-0.21	0.18
n = 9	PAR	**-0.89**	**-0.86**	**0.64**	0.45	**-0.82**
SBC	NO_3	**0.69**	**0.71**	**-0.25**	-0.02	**0.50**
n = 111	PAR	**-0.24**	**-0.21**	**0.29**	0.04	**-0.28**
San Diego	NO_3	0.39	0.24	-0.39	-0.99	**1.00**
n = 9	PAR	-0.03	0.02	0.35	-0.67	0.06

Figure 3.1. Time series of (a) seawater nitrate concentrations (5 day mean), and (b) photosynthetically active radiation (PAR; 15 day mean) at each site. Time series of (c) chlorophyll *a* (Chl*a*), (d) fucoxanthin (FX), (e) chlorophyll to carbon ratio (Chl:C), and (f) carbon content taken from 15 samples at each of the five study sites: Santa Cruz (SC), Arroyo Quemado (AQ), Arroyo Burro (AB), Mohawk (MO), San Diego (SD).
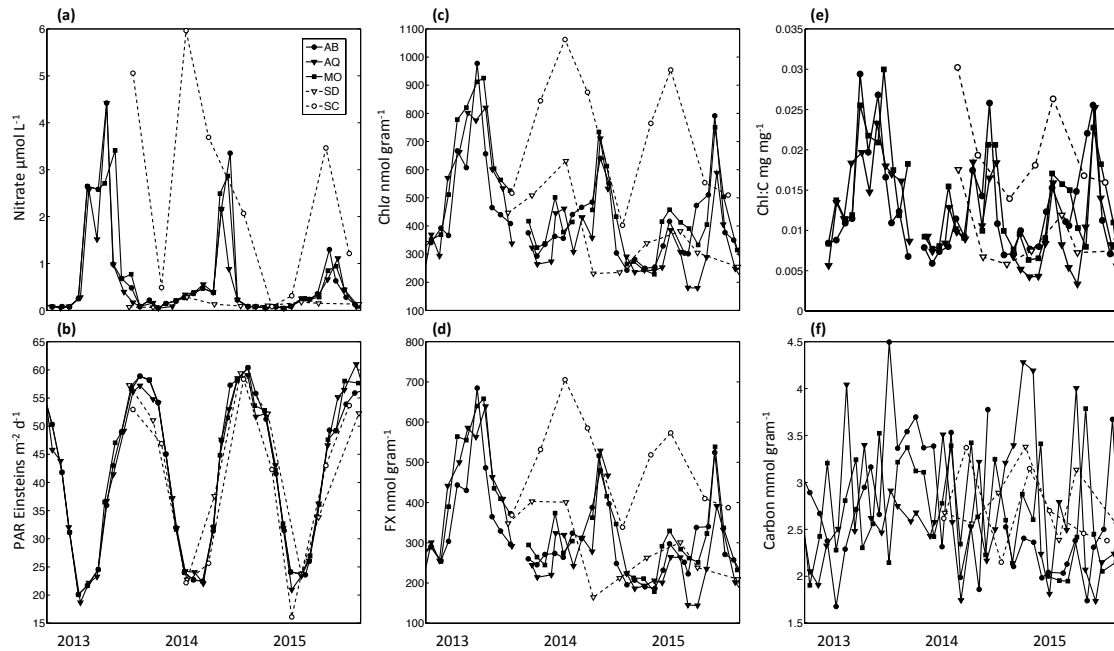
Figure 3.2. Non-linear additive effect curves of (a) seawater nitrate concentration and (b) photosynthetically active radiation (PAR) on the chlorophyll to carbon ratio of giant kelp canopy blades across all sites. The solid line is the mean effect of the predictor and the shaded regions represent the 95% confidence interval. The frequency of each predictor variable through space and time is shown as the black histogram at the bottom of each plot.
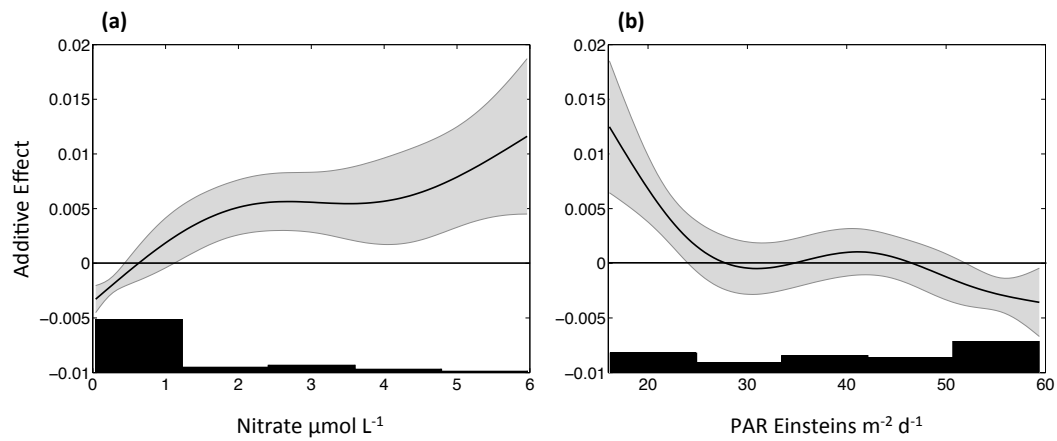
Figure 3.3. Canopy biomass of the 30 closest Landsat pixels (30 x 30 m) to the study site (left) and residuals of the 3-month temporal autocorrelation function (right; solid line) and chlorophyll to carbon ratio (right; dashed line) for the five study sites: (a) Santa Cruz (SC), (b) Arroyo Quemado (AQ), (c) Arroyo Burro (AB), (d) Mohawk (MO), (e) San Diego (SD). Pearson correlation coefficients (r) and calculated probabilities (p) reported for residuals and chlorophyll to carbon ratio (one month lag for Arroyo Quemado and Mohawk; two month lag for Arroyo Burro) for each site through time.
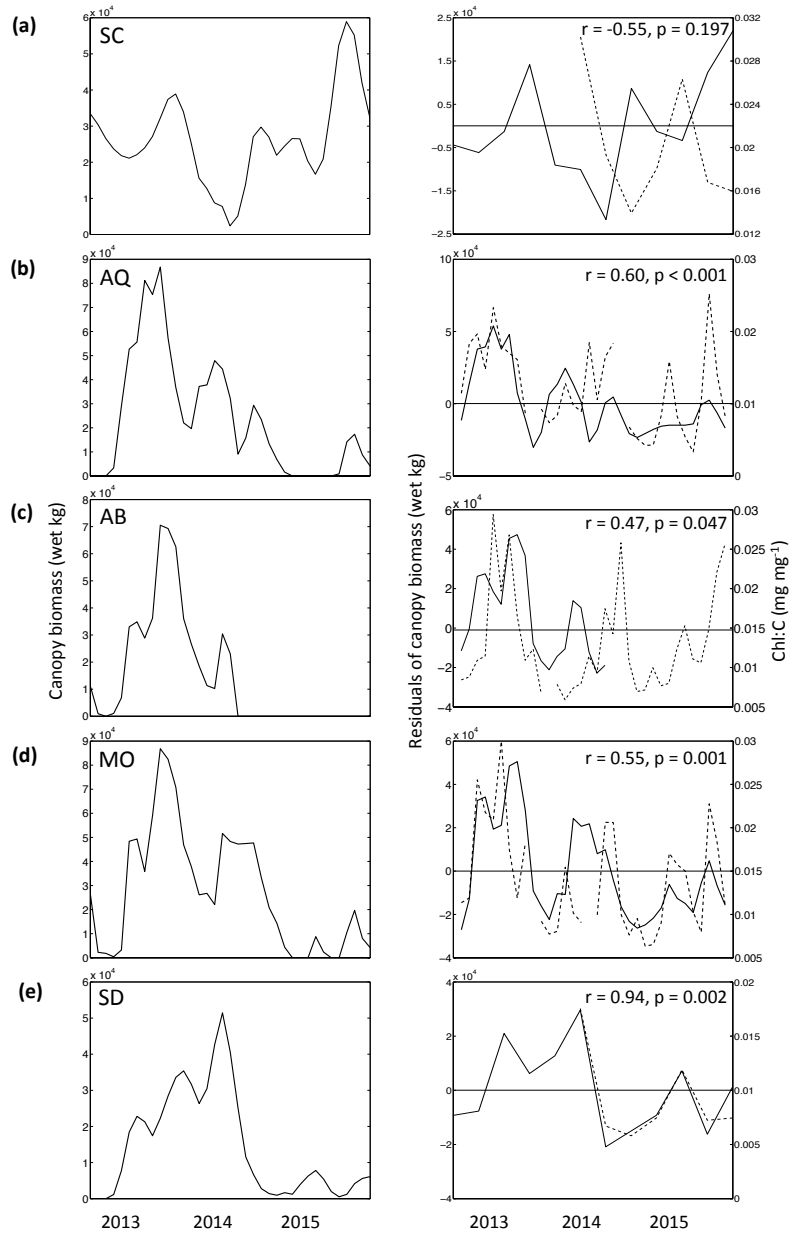
Figure 3.4. The top row shows diver estimated standing foliar crop (SFC; solid line) and chlorophyll to carbon ratio (Chl:C; dashed line) time series for each site in the Santa Barbara Channel, Arroyo Quemado (AQ), Arroyo Burro (AB), and Mohawk (MO). The bottom row shows net primary production (NPP) estimated from Santa Barbara Coastal Long Term Ecological Research project diver data at multiple time points (solid line) and modeled net primary production from present time SFC and Chl:C with a six month lag (dashed line). The statistics represent the Pearson correlation coefficients (r) and calculated probabilities (p) between the diver data based NPP model and the model which incorporates SFC and Chl:C at a single time point.
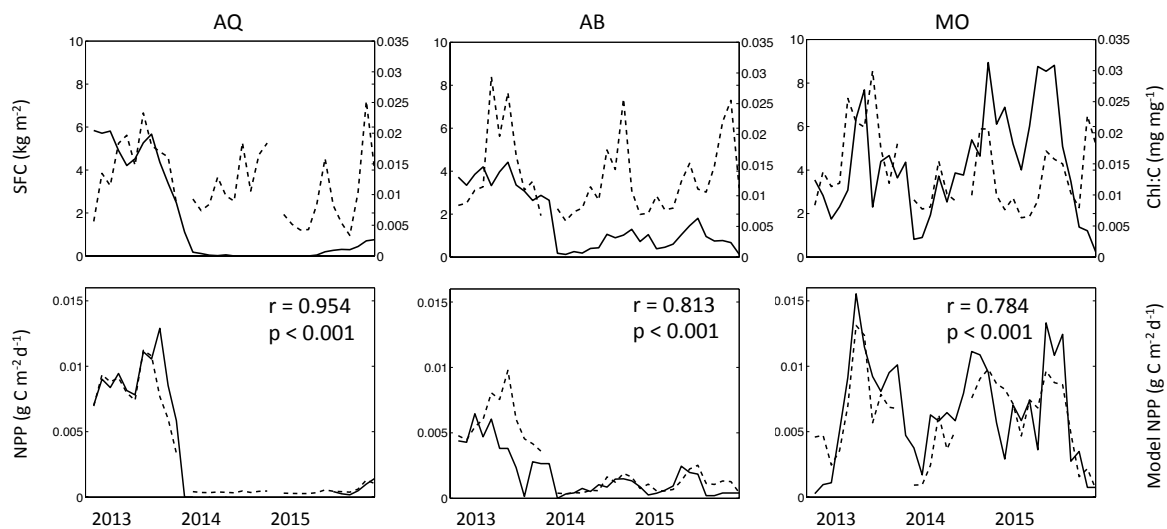
Figure 3.5. Additive effect curves of (a) standing foliar crop and (b) chlorophyll to carbon ratio (Chl:C) on the net primary production of giant kelp across the three sites in the Santa Barbara Channel. The solid line is the mean effect of the predictor and the shaded regions represent the 95% confidence interval. The frequency of each predictor variable through space and time is shown as the black histogram at the bottom of each plot.
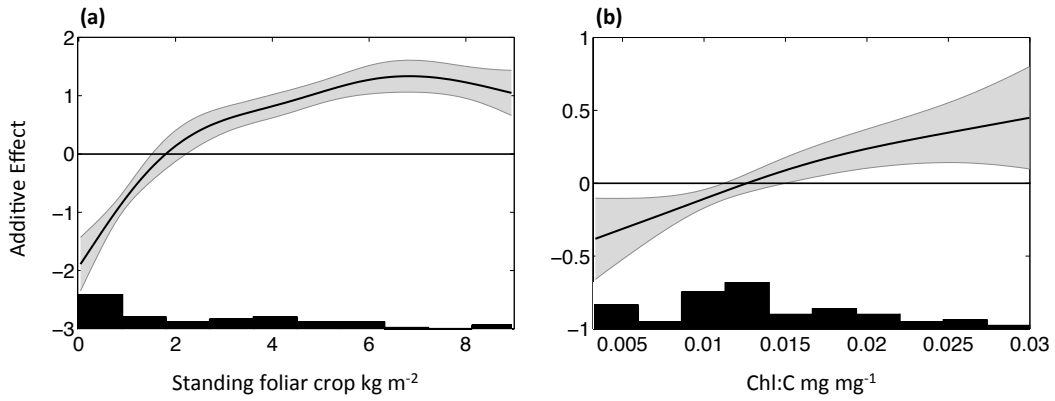
IV. Scale dependence of bottom-up vs. demographic control on the dynamics of giant kelp forests

Abstract

Examining patterns at a variety of scales is essential for identifying and elucidating ecological processes. In order to examine these patterns, it is essential to have high-resolution, spatially explicit data, which are becoming more available with advances in remotely sensed imagery. Giant kelp (*Macrocystis pyrifera*) is a foundation species that supports an economically important and ecologically diverse ecosystem on shallow reefs in temperate seas throughout the world. While regional scale control of giant kelp has been linked to environmental drivers, local growth rate and canopy biomass dynamics often defy these regional patterns. We examined changes in giant kelp canopy biomass and the chlorophyll *a* to carbon ratio (Chl:C; our proxy for physiological condition) in the Santa Barbara Channel using a time series of airborne hyperspectral imagery. We found that regional patterns of Chl:C were associated with large-scale fluctuations in sea surface temperature, and by extension ambient nutrient concentration. Local scale variability in Chl:C across a single kelp forest equaled the variability regionally, implying that local scale processes also play a role in the physiological condition of this species. Local scale examples showed that canopy Chl:C was related to the date when kelp canopy first emerged, suggesting that demographic patterns in kelp frond age influence the local physiological condition and persistence of giant kelp canopy.

A. Introduction

Ecological processes act at a variety of temporal and spatial scales to generate patterns that may or may not occur at the same scale at which those processes act (e.g., Levin 1992). For example, changes in climate can act to shift a species' distribution. However, the movement of the species may depend on the local scale cohesion of habitat patches, where areas of low cohesion may act to inhibit movement of the species in the climatically influenced direction (Opdam & Wascher 2004). Furthermore, these shifts in climate may increase disturbance effects and further fragment the habitat, leading to lower habitat cohesion and greater local control of the species' movements. Here we have two distinct processes acting on two scales, one on the continental and one on the local, with the larger scale process creating a positive feedback on the local scale process. If an observer were to ignore the local scale patterns in habitat fragmentation, the general pattern of species movement in response to climate change may be missed, and may even show the lowest amount of movement in the areas where shifts in climate are having the greatest effects. In order to elucidate these complex and potentially interacting processes it is important to examine pattern across a range of spatial scales.

In order to examine these patterns across space, it is essential to possess spatially extensive high-resolution data, which until recently has been rare in ecological studies. Over the past two decades there have been huge advances in environmental sensing, with exponential growth in ground-based meteorological and atmospheric gas flux towers, cheap and accurate global positioning systems, and increased availability of remotely sensed imagery (reviewed in Chave 2013). These technological advances have perhaps served

researchers the best in systems that are the most inaccessible. Asner et al. (2016) used a combination of hyperspectral imagery and coaligned light detection and ranging data to observe the spatial patterns of foliar nitrogen, phosphorus, and leaf mass per area across the Peruvian Amazon. From these spatial patterns, it was clear that elevation and substrate type were the two driving factors of these leaf trait distributions, and that these factors could strongly mediate trade-offs in leaf economic theory, such as resource acquisition versus storage. Understanding the importance of these processes at different spatial scales is key to predicting how these systems will change in the future.

The subtidal marine macroalga *Macrocystis pyrifera* (hereafter giant kelp) is a globally distributed foundation species that supports an incredibly productive ecosystem (Dayton 1985; Leet et al. 2001). Mature individuals consist of many vine-like fronds that possess leaf-like blades buoyed by pneumatocysts that enable the fronds to grow vertically in the water column to produce a canopy at the sea surface where it can take advantage of the high light environment. Giant kelp populations and biomass are dynamic and are influenced by environmental forcings such as upwelled nutrients and wave disturbance; however the relative importance of these drivers varies considerably across space (Reed et al. 2008; Reed et al. 2011; Bell et al. 2015a). Losses due to grazing can also have considerable impacts on giant kelp biomass and performance (Harrold & Reed 1985; Davenport & Anderson 2007). While external environmental drivers are important, intrinsic demographic processes such as frond senescence have been shown to be an important predictor of biomass dynamics (Rodriguez et al. 2013).

Physiological factors such as changes in the chlorophyll *a* to carbon ratio (Chl:C), our proxy for physiological condition, scale with growth rate for phytoplankton and juvenile sporophytes of giant kelp under nutrient-limited experimental cultures (e.g., Geider 1987; Shivji 1984). At larger scales, changes in Chl:C are associated with canopy biomass accumulation patterns and net primary production dynamics (Bell et al. *in prep*). In southern California, the Chl:C of growing giant kelp fronds is primarily associated with changes in nutrient concentrations associated with seasonal upwelling patterns; however fluctuations in giant kelp growth rate and canopy biomass often do not follow seasonal patterns of nutrient availability (Reed et al. 2008; Brzezinski et al. 2013; Bell et al. 2015a).

The idea of examining fluctuations in giant kelp systems across a variety of spatial scales is not new. Edwards (2004) examined the disturbance effect of the 1997/1998 El Niño event on giant kelp populations over five spatial scales ranging from a few meters to hundreds of kilometers. He found that the event acted across all spatial scales resulting in the loss of giant kelp throughout much of the NE Pacific, but that recovery was variable across scales. Giant kelp also displays spatially synchronous population dynamics over both local and regional scales (Cavanaugh et al. 2013). By contrasting these scales with those of known population drivers, it can be inferred that nutrients associated with ocean temperature and wave disturbance exert a greater pressure on giant kelp synchrony patterns across regional scales, while herbivory by sea urchins and kelp recruitment are more important on local scales. Demographic patterns associated with progressive frond senescence have been shown to be a better predictor of frond loss than external environmental factors (Rodriguez et al. 2013). While this has been shown to be a primary driver on the plot scale, there has been little published evidence of senescence patterns on larger spatial scales.

74

In this study, we take advantage of a novel remotely sensed dataset to examine patterns in giant kelp canopy physiological condition (Chl:C) across local and regional spatial scales. We aim to answer these two overarching questions: (1) What are the regional patterns of Chl:C and how are these related to the spatiotemporal patterns of environmental variables? (2) Are there local patterns in Chl:C and do these patterns relate to kelp forest growth and decline?

B. Methods

1. Site Description

Changes in physiological condition and giant kelp canopy biomass were examined in the Santa Barbara Channel (SBC), California, USA, which comprises the mainland coast of California from Point Arguello in the west to Point Dume in the east, as well as the four Northern Channel Islands. This area lies within the California Current System, where cool, relatively fresh waters are moved equatorward offshore to the west of the SBC, while warm, saline waters are moved into the eastern parts of the SBC by the inshore California Countercurrent (Hickey 1979; Lynn & Simpson 1987). Equatorward winds drive upwelling north of Pt. Conception during the spring and summer along with an intensification of the California Current (Huyer 1983; Lynn & Simpson 1987). This recently upwelled water is advected into the SBC from the west, and along with locally upwelled waters, provides uniform cool temperatures across the study region. A temperature gradient is formed across the length of the SBC during the early summer when warm water from the Southern California Bight is advected into the SBC from the east while cooler waters are upwelled in the west (Otero & Siegel 2004). Increased poleward flow and seasonal warming leads to

75

warm temperatures across the SBC during the late summer and fall. While this seasonal

pattern generally describes the observed ocean temperatures in the SBC, there can be

significant interannual variability, usually associated with oceanographic oscillations such as

the North Pacific Gyre Oscillation or El Niño Southern Oscillation, or large warming events

like the North East Pacific Warm Anomaly (Di Lorenzo et al. 2008; Chelton et al. 1982;

Bond et al. 2015, Reed et al. *in review*).

In the California Current System, changes in ocean temperature are inversely related

to nutrient concentrations, and are associated with spatial patterns of phytoplankton

productivity (Zimmerman & Kremer 1984; Palacios et al. 2013; Otero & Siegel 2004;

Henderikx Freitas et al. *in review*). Giant kelp grows on the rocky reefs which line the

shallow (<30m) margins of the SBC. These nutrient distributions and their onshore transport

are important for the growth and persistence of this macroalga and its associated ecosystem

(Wheeler & North 1980; Zimmerman & Kremer 1984). The majority of inorganic nitrogen

delivered to the inner shelf is related to local upwelling and the advection of recently

upwelled water into the SBC, with semidiurnal, vertical movements of nitrogen from

internal waves becoming an important source during the summer months (McPhee-Shaw et

al. 2007; Fram et al. 2008). Nitrogen inputs from terrestrial runoff only become an important

source during winter storms (McPhee-Shaw et al. 2007; Romero et al. 2016).

2. Environmental Data

In order to examine spatiotemporal changes in ocean temperature in the SBC, we

produced a time series of sea surface temperature (SST) at a spatial resolution of 4 km from

the MODIS Aqua satellite sensor (oceandata.sci.gsfc.nasa.gov). The mean SST for each 8-

day period was assessed for the study period (June 2012 - December 2015). Longer scale climatology (1982 – 2015) was produced using the National Climatic Data Center Optimal Interpolation Sea Surface Temperature data, which combines measurements from several sources including ship, buoys and Advanced Very High Resolution Radiometer (AVHRR) satellite images to produce a daily averaged dataset with a spatial resolution of 0.25° (Figure 1a). To assess differences in temperature across the SBC with this dataset, we compared the western-most pixel to the eastern-most pixel within to the channel (Figure 1b).

3. Estimates of Kelp Canopy Emergence

In order to track the progression of giant kelp canopy development, we estimated the approximate date of canopy emergence using Landsat 7 Enhanced Thematic Mapper Plus and Landsat 8 Operational Land Imager satellite imagery. The combination of these two sensors delivers an image every eight days, with a usable cloud-free image about once per month. We defined the date of canopy emergence as the first date where kelp canopy biomass was observed in an image. Landsat multispectral imagery has been used to successfully estimate the canopy biomass of giant kelp across the NE Pacific, and has been validated across several Landsat sensors (detailed methods in Cavanaugh et al. 2011; Bell et al. *in prep*). Briefly, images are atmospherically corrected and radiometrically standardized to a reference image using at least 50 temporally stable pseudo-invariant targets. Each pixel is then modeled as a linear combination of one temporally stable giant kelp canopy endmember and one of 30 temporally varying seawater endmembers, which are unique to each image date, using Multiple Endmember Spectral Mixing Analysis (MESMA; Roberts et al. 1998). The fractional cover of kelp canopy in each pixel was compared to diver

77

estimated kelp canopy biomass at two sites in the SBC measured by the Santa Barbara

Coastal Long Term Ecological Research Project (SBC LTER) from 2002 – 2015 (r^2 = 0.624,

p < 0.001, Bell et al. *in prep*).

4. Laboratory Analysis of Kelp Canopy Physiological Condition

We assessed giant kelp canopy physiological condition and biomass at three sites in

the SBC, Arroyo Quemado (34.4677 N, 120.1191 W), Arroyo Burro (34.4003 N, 119.7446

W), and Mohawk (34.3941 N, 119.7296 W) kelp forests. These sites were sampled monthly

from August 2012 – August 2015. Fifteen mature blades were collected haphazardly from

different plants inside a permanent 40 x 40m plot at each site. The blades were standardized

for age by collecting approximately two meters from the tip of an actively growing frond.

Blades were placed in a sealed plastic bag which was immediately placed on ice in an

opaque cooler. The blades were then transported to the lab where they were stored at 4°C

until being processed within 24 hours of collection.

A 5 x 5cm square was cut from the center of each blade approximately 5cm

above the pneumatocyst. The reflectance of the square was then measured between

350 – 800nm, at 1nm intervals, using a Shimadzu UV 2401PC spectrophotometer with

an integrating sphere attachment. Chlorophyll *a* concentrations were determined from

a 0.8 cm^2 disc excised from the center of each square. Each disc was weighed and placed in

4mL of dimethyl sulfoxide for 45 minutes at room temperature in the dark. The disc was

then removed and washed with 1mL water before being placed in 5mL of a 3:1:1 acetone,

methanol, and water solution for 2 hours at 4°C in the dark (following Seely et al. 1972).

The extracts were placed in individual quartz cuvettes and absorbance was measured in the

visible range using the spectrophotometer. Chlorophyll *a* concentration was determined

using absorbance based equations (Seely et al. 1972). A separate 5cm^2 disc was excised

from each blade near the pneumatocyst and rinsed in a 10% HCl solution. These discs were

weighed and combined for each site and date before being placed in a drying oven at 60°C

for several days, after which, dry mass was recorded. The dried discs were ground to a fine

powder and analyzed for carbon and nitrogen content using an elemental analyzer (Carlo-

Erba Flash EA 1112 series, Thermo-Finnigan Italia, Milano, Italy). Chl:C was calculated by

dividing the molar mass of chlorophyll *a* by the dry mass of carbon for each disc.

5. *Hyperspectral Estimates of Kelp Canopy Physiological Condition*

Bell et al. (2015b) developed an algorithm to determine kelp blade Chl:C from

laboratory reflectance. The mean 1nm reflectance intervals for each site date were degraded

to ~10nm bands consistent with the Airborne Visible Infrared Imaging Spectrometer

(AVIRIS). Briefly, the change between band's reflectance value was calculated to be the

first derivative of pseudoabsorbance $\delta(\ln 1/R)$, where R is the reflectance of each band

(Yoder & Pettigrew-Crosby 1995). These spectral slopes were correlated to their

corresponding mean measured Chl:C for each site date. The optimal spectral predictor of

blade Chl:C was the first derivative of pseudoabsorbance between bands centered at 658 and

677nm using an exponential relationship (Equation 1).

Eq. 1 $$Chl:C = 0.0353e^{-7.53x}$$

where x is equal to the slope of pseudoabsorbance between the two bands. Cross validation analysis found that this relationship explained 76% of the observed variance in laboratory assessed Chl:C (Bell et al. 2015b).

The AVIRIS sensor provided hyperspectral imagery, each image with an 11km swath width, of the SBC approximately three times per year (April, June, August) from 2013 – 2015 as part of the HyspIRI Preparatory Airborne Campaign (http://hyspiri.jpl.nasa.gov/airborne). The AVIRIS sensor provides imagery of upwelling spectral radiance in 224 contiguous, 10nm bands (400-2500nm). For this study orthocorrected level 2 reflectance products were used. These images were provided at a spatial resolution of 18m and atmospherically corrected according to Thompson et al. (2015). All imagery are freely available (ftp://popo.jpl.nasa.gov/).

The giant kelp Chl:C algorithm was applied to the hyperspectral imagery of the SBC. One issue with scaling from kelp blade measurements in the laboratory to measurements of kelp canopy in the imagery was that each pixel is a mixture of giant kelp canopy and seawater. To account for differences in fractional cover between pixels, MESMA was used as described above to calculate the proportional kelp cover for each pixel. Only pixels with greater than 0.1 proportional kelp cover were used in the analysis. For each image date, each kelp pixel was normalized for proportional kelp cover using the empirical relationship between the difference in reflectance for the bands centered at 658 – 667nm and the fractional kelp cover in that pixel. Equation 1 was then applied to all imagery to estimate the Chl:C of each kelp pixel in the SBC for each image date. To validate the algorithm for floating giant kelp canopy, we compared field sampled Chl:C from each site to the mean

Chl:C of the four AVIRIS pixels that overlaid each site for the sampling date closest to each image acquisition. If an image date fell between two field sample dates (>5 days) the later sampling date was used to account for changing environmental conditions. Field and image estimated Chl:C were compared using a reduced major axis least squared regression (lsqfitgm function, Matlab 2013a).

6. Relationship of Kelp Physiological Condition to Environmental Variables and Canopy Emergence

To determine the relationship between SST and Chl:C estimated from hyperspectral imagery over regional scales, the coastline of the SBC was divided into 1km segments. All kelp pixels were binned into their closest coastline segment. If the coastline segment contained >100 classified kelp pixels, the mean of those pixels was calculated and assigned to that segment, for each image date. Each coastline segment was assigned a SST for each image date by taking the mean of all MODIS SST pixels within a 3.5km radius for the 8 day mean previous to the image date. Chl:C and SST for each segment were compared with each other in a linear fashion using a reduced major axis least squared regression for each image (lsqfitgm function, Matlab 2013a). Since the overall relationship among all dates may not be linear, a generalized additive model was used to elucidate the potentially non-linear fit using the mgcv package in R (Wood 2006).

Canopy emergence time was determined based on the date the kelp pixel was first observed before the AVIRIS flight. Each AVIRIS pixel was assigned an emergence date based on the emergence of its closest Landsat pixel. For each AVIRIS image date, pixels were grouped based on emergence date and the mean and standard error of the Chl:C

estimates for those pixels was determined. For canopy emergence to be determined, a particular kelp bed must have displayed no canopy biomass at least 120 days prior to the AVIRIS image acquisition date. Relationships between canopy Chl:C and emergence date were assess using reduced major axis least squared regressions (lsqfitgm function, Matlab 2013a).

C. Results

1. Environmental Variability

The SST in the SBC displayed a seasonal pattern of cool temperatures in the winter, followed by periodic cooling due to seasonal upwelling during the spring and early summer. Temperatures rose throughout the summer and into the fall as upwelling decreased, combined with increased insolation (Figure 1a). The upwelling period during 2013 occurred earlier in the year and was greater in magnitude than both 2014 and 2015, which were associated with a warm water anomaly and El Niño event, respectively. April and June images generally occurred during cool periods associated with upwelling patterns, while August images occurred during warm water periods. The western end of the SBC generally maintained cooler SST than the eastern end of the channel (Figure 1b). The temperature differences in the SBC tended to be greatest in June and July, maintaining the general pattern observed in the past. The last two years of the record (2014-2015) displayed higher than average SST consistent with the North East Pacific Warm Anomaly and El Niño event.

2. Validation of Physiological Condition Estimates from Hyperspectral Imagery

A total of eight AVIRIS missions were assembled for comparison to field determined Chl:C (Table 1). Due to clouds or lack of sufficient kelp canopy at the sites, a total of 15 field data/image comparisons were made out of a possible 24. The image estimated Chl:C was significantly related to the field estimates with a strong, positive linear relationship ($r^2 = 0.67$, $p < 0.0001$; Figure 2). The slope of the relationship was 0.98 (standard deviation = 0.16), with a y-intercept of -5.1×10^{-4} (standard deviation = 0.0026), close to a 1:1 relationship.

3. Relationship of Kelp Physiological Condition to Regional Environment

The regional patterns of Chl:C for each 1 km coastline segment and SST for each image are shown in Figure 3. Generally, Chl:C of the canopy is higher when the SST adjacent to that canopy is cooler, and Chl:C is lower when SST is warmer. When there is a gradient in SST across the SBC, we tend to observe an anticorrelated gradient in Chl:C of the giant kelp canopy on a 1km scale. The relationship between the coastline segments of mean Chl:C and mean SST are plotted as separate scatterplots with the best fit line determined by reduced major axis least squared regression (Figure 4). All images showed a negative, linear relationship except for the April 2015 ($p = 0.145$) and August 2014 ($p = 0.88$) image, which showed no significant relationship (Table 1; shown as best fit lines in Figure 3). The overall relationship across all images required a non-linear fit with a negative, linear relationship from 12 - 20°C transitioning to a near zero slope from 20 - 25°C ($r^2 = 0.63$, $p < 0.0001$).

83

4. Relationship of Kelp Physiological Condition to Local Canopy Emergence Pattern

There was considerable local-scale variation in canopy Chl:C and biomass across the study period. Within one image date there could be a 3-fold difference in canopy Chl:C, and these variations were not consistent through time (Figure 5). The relationship between Chl:C and days since canopy emergence were examined for six sites. These sites shared an initial state of zero kelp canopy at least 120 days before the date of the hyperspectral image acquisition in order to track the emergence patterns for the entire bed within the lifespan for a giant kelp frond. Spatial maps of canopy emergence and canopy Chl:C are presented in Figure 6, as well as the relationship between canopy emergence date and mean canopy Chl:C. Pixels were canopy had been observed earliest tended to have lower Chl:C, while canopy pixels that were first observed most recently tended to have higher Chl:C.

D. Discussion

1. Regional Patterns of Kelp Canopy Physiological Condition

Regional physiological condition of giant kelp canopy in the SBC changes through space and time. These changes in condition have implications for the growth and persistence of this foundation species as increases in the Chl:C are associated with biomass accumulation patterns in the Southern California Bight (Bell et al. *in prep*). On all but two dates, the regional patterns of Chl:C in the SBC were negatively related to SST (Figure 4). On one of the dates when there was no relationship there were uniformly warm water temperatures across the SBC, with corresponding uniformly low canopy Chl:C (August 2014; Figure 3). The shape of the non-linear relationship comparing Chl:C to SST, across all

dates, closely resembles the SST vs. nitrate relationship (Figure 4). This relationship

generally shows a steep, negative decline in nitrate concentrations as temperatures rise to

about 15.5°C, at which point nitrate concentrations are about 1 µmol L^{-1}, which then

decrease at more gradual rate. The Chl:C of giant kelp and other marine flora generally

increases in response to additional nitrogen when in a nutrient-limited environment, (Laws

& Bannister 1980; Bell et al. *in* prep). The relationship between Chl:C and SST begins to

flatten out when SST reaches about 20°C, a few degrees higher than the inflection point of

the temperature vs. nitrate concentration relationship. While giant kelp does have a limited

capacity for nitrogen storage, nitrogen content and elongation rate drop dramatically after

about 2 weeks in a low nutrient environment (Gerard et al. 1982). A more probable

explanation is that giant kelp obtains a significant proportion of inorganic nitrogen through

semi-diurnal internal waves during the summer months (Zimmerman & Kremer 1984;

McPhee-Shaw et al. 2007; Fram et al. 2008; Brzezinski et al. 2013). These regular

incursions of cool, nutrient-rich water onto the inner shelf provide a seasonal source of

inorganic nitrate that may be masked by a stratified water column with warm surface

temperatures.

The similarity of the relationship between Chl:C and SST and between nitrate

concentration and SST implies that the mean Chl:C of a kelp forest is determined by the

nutrient concentrations in the surrounding water column. This has several implications for

the growth and persistence of giant kelp across this region. Higher ambient nutrient

concentrations have been associated with increased photosynthetic pigments and frond

elongation rates (Kopczak 1994; Zimmerman & Kremer 1984). Increases in the Chl:C have

been linked to increased growth rates in juvenile sporophytes and canopy biomass

85

accumulation (Shivji 1984; 1985; Bell et al. *in prep*). Furthermore increases in available nutrients increase spore production, elevating the probability of successful recruitment (Reed et al. 1996). However despite this clear regional pattern, there was often a large variation in the canopy Chl:C within a single kelp forest (Figure 6). The scatter about each best fit line and the offset of each image's line from the mean relationship suggest that local scale factors also play a role in the physiological condition of this species.

2. Local Scale Canopy Physiological Condition as a Demographic Process

The variability in Chl:C across a single kelp forest may display a range equal to that seen across the entire SBC (Figures 3, 5). However, there is little evidence to suggest that kelp forests uptake inorganic nitrogen at rates fast enough to be responsible for this nutrient gradient. Fram et al. (2008) found that, in a moderately sized kelp forest, the residence time of seawater moving through the forest was short, so ambient concentrations of nitrate were not affected by upstream kelp, and that uptake was primarily governed by uptake kinetics and not mass transfer. Furthermore, in the Point Loma kelp forest off of San Diego, CA, USA (one of the largest kelp forests in the world) nutrient concentrations inside the forest were not depleted by the kelp or enhanced by sediment regeneration, which implies fast exchange between water inside and outside of the kelp forest (Jackson 1977). Yet, variability in canopy Chl:C appears to exist and must be the result of a different process.

Progressive senescence processes may provide a better explanation of the dynamics of giant kelp fronds than extrinsic environmental forcings in the SBC (Rodriguez et al. 2013). These internal biological processes may be especially important for giant kelp biomass dynamics as fronds make up 95% of the plant's biomass and all of the canopy's

biomass (Rodriguez et al. 2013; North 1994). Fronds produce blades at the apical meristem, which is lost as the frond ages, ceasing blade production and initiating senescence (Lobban 1978). Blades are the principle light harvesting structures on the frond and the maximum photosynthetic rate and nitrogen content decrease as a function of age (Wheeler 1980; Rodriguez et al. 2016). Because of the strong relationship between blade nitrogen content and Chl:C, as well as the links between Chl:C and growth rate through enhanced photosynthesis under high light conditions, it is logical to assume that Chl:C decreases as a function of blade age (Shivji 1984).

The spatial patterns of Chl:C estimated from hyperspectral imagery are related to the spatial patterns of canopy emergence (Figure 6). Canopy emergence shows growth starting in the center of the bed with new growth towards the edges. The oldest parts of the canopy tend to have the lowest Chl:C, with newer areas displaying higher values. Since the kelp at the edges represents new growth, it would follow that the fronds of these plants were actively growing and had not yet begun to senesce. The microscopic stages of giant kelp have high light requirements and are vulnerable to intra-specific competition through shading (Schiel & Foster 2006). In a kelp bed with developed canopy, the edges would represent the highest light environment and an optimal area to recruit. The spatial patterns of Chl:C in relation to the timing of canopy emergence allow for the deduction of a conceptual model of canopy growth and senescence (Figure 7). Each remote sensing pixel represents an average Chl:C of all canopy fronds within it. When new giant kelp canopy emerges, it will be comprised of all actively growing fronds whose Chl:C is a product of the regional nutrient and light environment. As these fronds age, they will lose their apical meristem, becoming a terminal frond, and cease the production of new blades. The blades on these

aging fronds will begin to senesce with reductions in photosynthetic performance and Chl:C. Simultaneously new growing fronds emerge but since the canopy is mixture of growing, terminal, and senescent fronds there will be a depression in the mean Chl:C for that pixel. As canopy ages, terminal and senescent fronds become a higher proportion of canopy biomass until the addition of new growing fronds equals frond loss through the process of progressive senescence (Rodriguez et al. 2013). As environmental conditions change, there will be changes in the frond initiation rate, shifting the proportion of new growing fronds in relation to terminal and senescent fronds in the canopy. If there is a cessation in the initiation of growing fronds only terminal and senescent fronds will form the canopy which will further depress the mean Chl:C and lead to eventual canopy loss (Figure 5). This loss of the kelp forest canopy represents not only a loss of photosynthetic material in a high light environment essential to the production of new fronds, but a loss of three dimensional structure for the species of the kelp forest ecosystem (Jackson 1987; North 1994). This structure serves as habitat to many reef fishes and serve as important recruitment sites for many fish and invertebrates (Carr 1989; 1991; Anderson 1994; Holbrook et al. 1990; Morton et al. 2013).

3. Importance of Environment to the Detection of Process

Starting in late 2013, the NE Pacific was subject to an anomalous warming event that is unprecedented in the instrumental record (Bond et al. 2015). This event was immediately followed by one of the strongest El Niño events ever recorded. The SBC was subjected to high SST and low nutrient concentrations during this two-year period with brief upwelling events to stimulate productivity (Figure 1a; Reed et al. *in review*). One of the unexpected

opportunities to arise from this quick succession of extreme events was a natural experiment in the examination of giant kelp canopy growth and senescence patterns. Most kelp canopy was lost near the end of 2014 after a summer and fall of anomalously low seawater nutrient concentrations, which presumably led to low or nonexistent frond initiation rates. The onset of the spring upwelling in April 2015 led to a brief regrowth of kelp canopy, especially in the western part of the SBC where SST was reduced. This regrowth period was followed by another summer of high temperatures and low nutrient availability and subsequent canopy loss. This period of canopy emergence, growth, and decline of many kelp forests in the SBC was captured by three hyperspectral images (Figure 5). The absence of canopy in early 2015 also allowed for an initial canopy emergence date for each pixel before the hyperspectral flights. Without this starting point it would have been impossible to construct canopy emergence maps as most giant kelp patches can persist for years in the Southern California Bight (Castorani et al. 2015). Simultaneous losses of frond cohorts have been observed at plot scales in the past, but the reset of giant kelp canopy driven by regional changes in the environment, along with multiple acquisitions of hyperspectral imagery unveiled a process showing how senescence and demographic structure can influence canopy dynamics on local scales.

4. Future of Remotely Sensed Physiological Condition

The recent revolution in the processing speed, storage, and quantity of freely available remotely sensed imagery has allowed researchers to examine ecological questions over vast spatial and temporal scales (Goetz 2009; Wulder et al. 2012). One area of research that has led to multiple advances has been the estimation of giant kelp biomass dynamics

across the NE Pacific using Landsat (Cavanaugh et al. 2011; 2013; 2014; Bell et al. 2015a; Castorani et al. 2015; *in review*; Young et al. 2016). While multispectral imagery, like Landsat, can provide estimates of giant kelp canopy quantity, the measurement of numerous, continuous bands from hyperspectral sensors allows for the estimation of canopy quality (Bell et al. 2015b). The addition of physiological condition to biomass furthers our understanding of the spatial scales of production for this foundation species, which may help us understand its role in structuring the ecosystem which depends on it (Bell et al. *in prep*; Morton et al. 2016). The future of hyperspectral remote sensing involves moving from a mission based airborne sensor to a spaceborne sensor, capable of providing global, repeat imagery. The Hyperspectral Infrared Imager (HyspIRI) is a planned mission that will provide this imagery for a multitude of physiological, ecological, and geological uses (https://hyspiri.jpl.nasa.gov/; Lee et al. 2015; Hochberg et al. 2015). If only applied to giant kelp forests, using already developed algorithms, researchers could track changes in biomass, Chl:C, and canopy progression globally, all from the same images. Indeed, hyperspectral remote sensing will allow for many traits to be quantified simultaneously across ecosystems, and repeat imagery will monitor change in these traits on global scales.

E. Chapter Acknowledgements

F. Literature Cited

Anderson, T. W. 1994. Role of macroalgal structure in the distribution and abundance of a temperate reef fish. Mar. Ecol. Prog. Ser. **113**: 279–290.

Asner, G. P., D. E. Knapp, C. B. Anderson, R. E. Martin, and N. Vaughn. 2016. Large-scale climatic and geophysical controls on the leaf economics spectrum. Proc. Natl. Acad. Sci. U. S. A. **113**: 4043–4051. doi:10.1073/pnas.1604863113

Bell, T.W., J. Allen, K. C. Cavanaugh, and D.A. Siegel. *in prep*. Multidecadal views of giant kelp forests off California from the Landsat satellites.

Bell, T. W., K. C. Cavanaugh, D. C. Reed, and D. A. Siegel. 2015. Geographical variability in the controls of giant kelp biomass dynamics. J. Biogeogr. **42**: 2010–2021. doi:10.1111/jbi.12550

Bell, T. W., K. C. Cavanaugh, and D. A. Siegel. 2015. Remote monitoring of giant kelp biomass and physiological condition: An evaluation of the potential for the Hyperspectral Infrared Imager (HyspIRI) mission. Remote Sens. Environ. **167**: 218–228. doi:10.1016/j.rse.2015.05.003

Bell, T. W., D. C. Reed, and D. A. Siegel. *in prep.* Giant kelp biomass and net primary productivity dynamics are associated with regional patterns of physiological condition. Limnol. Oceanogr.

Bond, N. A., M. F. Cronin, H. Freeland, and N. Mantua. 2015. Causes and impacts of the 2014 warm anomaly in the NE Pacific. Geophys. Res. Lett. **42**: 3414–3420. doi:10.1002/2015GL063306.Received

Brzezinski, M., D. Reed, S. Harrer, A. Rassweiler, J. Melack, B. Goodridge, and J. E. Dugan. 2013. Multiple Sources and Forms of Nitrogen Sustain Year-Round Kelp Growth on the Inner Continental Shelf of the Santa Barbara Channel. Oceanography **26**: 114–123.

Carr, M. H. 1991. Habitat selection and recruitment of an assemblage of temperate zone reef fishes. J. Exp. Mar. Bio. Ecol. **146**: 113–137.

Carr, M. H. 1989. Effects of Macroalgal Assemblages on the Recruitment of Temperate Zone Reef Fishes. J. Exp. Mar. Bio. Ecol. **126**: 59–76.

Castorani, M. C. N., D. C. Reed, F. Alberto, T. W. Bell, R. D. Simons, K. C. Cavanaugh, D. A. Siegel, and P. T. Raimondi. 2015. Connectivity structures local population dynamics: A long-term empirical test in a large metapopulation system. Ecology **96**: 3141–3152.

Castorani, M. C. N., D. C. Reed, P. T. Raimondi, F. Alberto, T. W. Bell, K. C. Cavanaugh, D. A. Siegel, and R. D. Simons. *in review*. Fluctuations in population fecundity drive demographic connectivity and structure metapopulation dynamics. Proceedings of the Royal Society B.

Cavanaugh, K., B. Kendall, and D. Siegel. 2013. Synchrony in dynamics of giant kelp forests is driven by both local recruitment and regional environmental controls. Ecology **94**: 499–509.

Cavanaugh, K., D. Siegel, D. Reed, and P. Dennison. 2011. Environmental controls of giant-kelp biomass in the Santa Barbara Channel, California. Mar. Ecol. Prog. Ser. **429**: 1–17. doi:10.3354/meps09141

Cavanaugh, K. C., D. a Siegel, P. T. Raimondi, and F. Alberto. 2014. Patch definition in metapopulation analysis: a graph theory approach to solve the mega-patch problem. Ecology **95**: 316–28.

Chave, J. 2013. The problem of pattern and scale in ecology: what have we learned in 20 years? Ecol. Lett. 4–16. doi:10.1111/ele.12048

Chelton, D. B., P. A. Bemal, and J. A. Mcgowan. 1982. Large-scale interannual physical and biological interaction in the California Current. J. Mar. Res. **40**: 1095–1125.

Davenport, A. C., and T. W. Anderson. 2007. Positive indirect effects of reef fishes on kelp performance: the importance of mesograzers. Ecology **88**: 1548–61.

Dayton, P. 1985. Ecology of Kelp Communities. Annu. Rev. Ecol. Syst. **16**: 215–245.

Di Lorenzo, E., N. Schneider, K. M. Cobb, and others. 2008. North Pacific Gyre Oscillation links ocean climate and ecosystem change. Geophys. Res. Lett. **35**: L08607. doi:10.1029/2007GL032838

Edwards, M. 2004. Estimating scale-dependency in disturbance impacts: El Niños and giant kelp forests in the northeast Pacific. Oecologia **138**: 436–447. doi:10.1007/s00442-003-1452-8

Fram, J. P., H. L. Stewart, M. A. Brzezinski, B. Gaylord, D. C. Reed, S. L. Williams, and S. MacIntyre. 2008. Physical pathways and utilization of nitrate supply to the giant kelp, *Macrocystis pyrifera*. Limnol. Oceanogr. **53**: 1589–1603.

Geider, R. J. 1987. Light and temperature dependence of the carbon to chlorophyll a ratio in microalgae and cyanobacteria. New Phytol. **106**: 1–34. doi:10.1016/0198-0254(87)96047-X

Gerard, V. 1982. Growth and utilization of internal nitrogen reserves by the giant kelp *Macrocystis pyrifera* in a low-nitrogen environment. Mar. Biol. **66**: 27–35.

Goetz, A. F. H. 2016. Three decades of hyperspectral remote sensing of the Earth: A personal view. Remote Sens. Environ. **113**: S5–S16. doi:10.1016/j.rse.2007.12.014

Harrold, C., and D. Reed. 1985. Food availability, sea urchin grazing, and kelp forest community structure. Ecology 66: 1160–1169.

Henderikx Freitas, F., E. Fields, S. Maritorena, and D. A. Siegel. *in review*. Satellite assessment of particulate matter and phytoplankton variations in the Santa Barbara Channel and its surrounding waters: role of surface waves. J. of Geophysical Research.

Hickey, B. M. 1979. The California Current System-hypotheses and facts. Prog. Oceanogr. **8**: 191–279.

Hochberg, E. J., D. A. Roberts, P. E. Dennison, and G. C. Hulley. 2015. Remote Sensing of Environment Special issue on the Hyperspectral Infrared Imager (HyspIRI): Emerging science in terrestrial and aquatic ecology, radiation balance and hazards. Remote Sens. Environ. **167**: 1–5. doi:10.1016/j.rse.2015.06.011

Holbrook, S. J., M. H. Carr, R. Schmitt, and J. A. Coyer. 1990. Effect of Giant Kelp on Local Abundance of Reef Fishes: The Importance of Ontogenetic Resource Requirements. Bull. Mar. Sci. **47**: 104–114.

Huyer, A. 1983. Coastal upwelling in the California current system. Prog. Oceanogr. **12**: 259–284. doi:10.1016/0079-6611(83)90010-1

Jackson, G. A. 1977. Nutrients and production of giant kelp, *Macrocystis pyrifera*, off southern California. Limnol. Oceanogr. **22**: 979–995.

Jackson, G. 1987. Modelling the growth and harvest yield of the giant kelp *Macrocystis pyrifera*. Mar. Biol. **624**: 611–624.

Kopczak, C. D. 1994. Variability of Nitrate Uptake Capacity in *Macrocystis pyrifera* (Laminariales, Phaeophyta) with Nitrate and Light Availability. J. Phycol. **30**: 573–580.

Laws, E., and T. Bannister. 1980. Nutrient- and light-limited growth of Thalassiosira fluviatilis in continuous culture, with implications for phytoplankton growth in the ocean. Limnol. Oceanogr. **25**: 457–473.

Lee, C. M., M. L. Cable, S. J. Hook, R. O. Green, S. L. Ustin, D. J. Mandl, and E. M. Middleton. 2015. An introduction to the NASA Hyperspectral InfraRed Imager (HyspIRI) mission and preparatory activities. Remote Sensing of Environment. **167**: 6-19.

Leet, W.S., Dewees, C.M., Klingbeil, R., & Johnson, E.J. 2001. California's living marine resources: A status report. State of CA Resources Agency and Fish and Game (593 pp.).

Levin, S. A. 1992. The Problem of Pattern and Scale in Ecology : The Robert H . MacArthur Award Lecture. Ecology **73**: 1943–1967.

Lobban, C. S. 1978. The growth and death of the *Macrocystis* sporophyte (Phaeophyceae, Laminariales). Phycologia **17**: 196–212.

Lynn, R., and J. Simpson. 1987. The California Current SystemL The Seasonal Variability of its Physical Characteristics. J. Geophys. Res. **92**: 12947–12966.

McPhee-Shaw, E. E., D. A. Siegel, L. Washburn, M. A. Brzezinski, J. L. Jones, A. Leydecker, and J. Melack. 2007. Mechanisms for nutrient delivery to the inner shelf: observations from the Santa Barbara Channel. Limnol. Oceanogr. **52**: 1748–1766.

Morton, D. N., T. W. Bell, and T. W. Anderson. 2016. Spatial synchrony of amphipods in giant kelp forests. Mar. Biol. 1–11. doi:10.1007/s00227-015-2807-5

Morton, D. N., D. N. Morton, and T. W. Anderson. 2013. Spatial patterns of invertebrate settlement in giant kelp forests Spatial patterns of invertebrate settlement in giant kelp forests. Mar. Ecol. Prog. Ser. **485**: 75–89. doi:10.3354/meps10329

North, W. J. 1994. Review of *Macrocystis* biology. Pages 447– 527 in I. Akatsuka, editor. Biology of economic algae. SPB Academic, The Hague, The Netherlands. Ostfeld,

Opdam, P., and D. Wascher. 2004. Climate change meets habitat fragmentation: linking landscape and biogeographical scale levels in research and conservation. Biol. Conserv. **117**: 285–297. doi:10.1016/j.biocon.2003.12.008

Otero, M. P., and D. a. Siegel. 2004. Spatial and temporal characteristics of sediment plumes and phytoplankton blooms in the Santa Barbara Channel. Deep Sea Res. Part II Top. Stud. Oceanogr. **51**: 1129–1149. doi:10.1016/j.dsr2.2004.04.004

Palacios, D. M., E. L. Hazen, I. D. Schroeder, and S. J. Bograd. 2013. Modeling the temperature-nitrate relationship in the coastal upwelling domain of the California Current. J. Geophys. Res. Ocean. **118**: 3223–3239. doi:10.1002/jgrc.20216

Reed, D. C., A. Rassweiler, and K. K. Arkema. 2008. Biomass rather than growth rate determines variation in net primary production by giant kelp. Ecology **89**: 2493–2505. doi:10.1890/07-1106.1

Reed, D. C., A. Rassweiler, M. H. Carr, K. C. Cavanaugh, D. P. Malone, and D. A. Siegel. 2011. Wave disturbance overwhelms top-down and bottom-up control of primary production in California kelp forests. Ecology **92**: 2108–2116. doi:10.1890/11-0377.1

Reed, D. C., L. Washburn, A. Rassweiler, R. J. Miller, T. W. Bell. *in review*. Extreme warming challenges kelp forests as sentinels of climate change. Nature Communications.

Roberts, D., M. Gardner, and R. Church. 1998. Mapping chaparral in the Santa Monica Mountains using multiple endmember spectral mixture models. Remote Sens. … **65**: 267–279.

Rodriguez, G. E., D. C. Reed, and S. J. Holbrook. 2016. Blade life span, structural investment, and nutrient allocation in giant kelp. Oecologia. doi:10.1007/s00442-016-3674-6

Rodriguez, G., A. Rassweiler, D. Reed, and S. Holbrook. 2013. The importance of progressive senescence in the biomass dynamics of giant kelp (*Macrocystis pyrifera*). Ecology **94**: 1848–1858.

Romero, L., D. Siegel, J. McWilliams, Y. Uchiyama, and C. Jones. 2016. Journal of Geophysical Research : Oceans. J. Geophys. Res. Ocean. **121**: 3926–3943. doi:10.1002/2015JC011323.Received

Schiel, D. R., and M. S. Foster. 2016. The Population Biology of Large Brown Seaweeds: Ecological Consequences of Multiphase Life Histories in Dynamic Coastal Environments. Annu. Rev. Ecol. Evol. Syst. **37**: 343–372. doi:10.2307/annurev.ecolsys.37.091305.30000014

Seely, G., M. Duncan, and W. Vidaver. 1972. Preparative and analytical extraction of pigments from brown algae with dimethyl sulfoxide. Mar. Biol. **12**: 184–188.

Shivji, M. S. 1984. Physiological responses of juvenile *Macrocystis pyrifera* sporophytes (Phaeophyta) to environmental factors: light, nitrogen and the interaction of light and nitrogen. M.A. Thesis in Biology, University of California, Santa Barbara, 51 pp.

Shivji, M. 1985. Interactive effects of light and nitrogen on growth and chemical composition of juvenile *Macrocystis pyrifera* (L.) C. At. (Phaeophyta) sporophytes. J. Exp. Mar. Bio. Ecol. **89**: 81–96.

Thompson, D. R., B. Gao, R. O. Green, D. A. Roberts, P. E. Dennison, and S. R. Lundeen. 2015. Remote Sensing of Environment Atmospheric correction for global mapping spectroscopy: ATREM advances for the HyspIRI preparatory campaign. Remote Sens. Environ. **167**: 64–77. doi:10.1016/j.rse.2015.02.010

Wheeler, P., and W. North. 1980. Effect of Nitrogen Supply on Nitrogen Content and Growth Rate of Juvenile *Macocystis pyrifera* (Phaeophyta) Sporophytes. J. Phycol. **16**: 577–582.

Wheeler, W. 1980. Pigment content and photosynthetic rate of the fronds of *Macrocystis pyrifera*. Mar. Biol. **56**: 97–102.

Wood, S.N. 2006. Generalized Additive Models: An Introduction with R. Chapman and Hall/CRC.

Wulder, M. A., G. Masek, W. B. Cohen, T. R. Loveland, and C. Woodcock. 2012. Rem0te Sensing of Environment Opening the archive: How free data has enabled the science and monitoring promise of Landsat. Remote Sens. Environ. **122**: 2–10.

Yoder, B., and R. Pettigrew-Crosby. 1995. Predicting Nitrogen and Chlorophyll Content and Concentrations from Reflectance Spectra (400-2500 nm) at Leaf and Canopy Scales. Remote Sens. Environ. **53**: 199–211.

Young, M., K. Cavanaugh, T. Bell, P. Raimondi, C. A. Edwards, P. T. Drake, L. Erikson, and C. Storlazzi. 2016. Environmental controls on spatial patterns in the long-term persistence of giant kelp in central California. Ecol. Monogr. **86**: 45–60.

Zimmerman, R. C., and J. N. Kremer. 1984. Episodic nutrient supply to a kelp forest ecosystem in Southern California. J. Mar. Res. **42**: 591–604. doi:10.1357/002224084788506031

Table 4.1. The slopes and offset (y-intercept) for each best fit line between chlorophyll *a* to carbon ratio (Chl:C) for each 1km coastline segment and sea surface temperature for each image date. Correlation coefficients are also shown. * = p < 0.05 and ** p < 0.01.

Image	Slope	Offset	Correlation coefficient
April 11, 2013	-0.0038	0.0702	-0.6764**
June 6, 2013	-0.0037	0.0722	-0.5142*
April 16, 2014	-0.0016	0.0454	-0.6000*
June 6, 2014	-0.0041	0.0809	-0.7163**
August 29, 2014	0.0007	-0.0099	0.0178
April 16, 2015	-0.0025	0.0628	-0.6657
June 2, 2015	-0.0048	0.0902	-0.3419*
August 24, 2015	-0.0030	0.0689	-0.3844*

Figure 4.1. (a) Monthly mean sea surface temperature (SST) for the Santa Barbara Channel (SBC) and (b) difference in SST between the western and eastern ends of the SBC. Line plots show means for each year 1982 – 2015 and means among months.
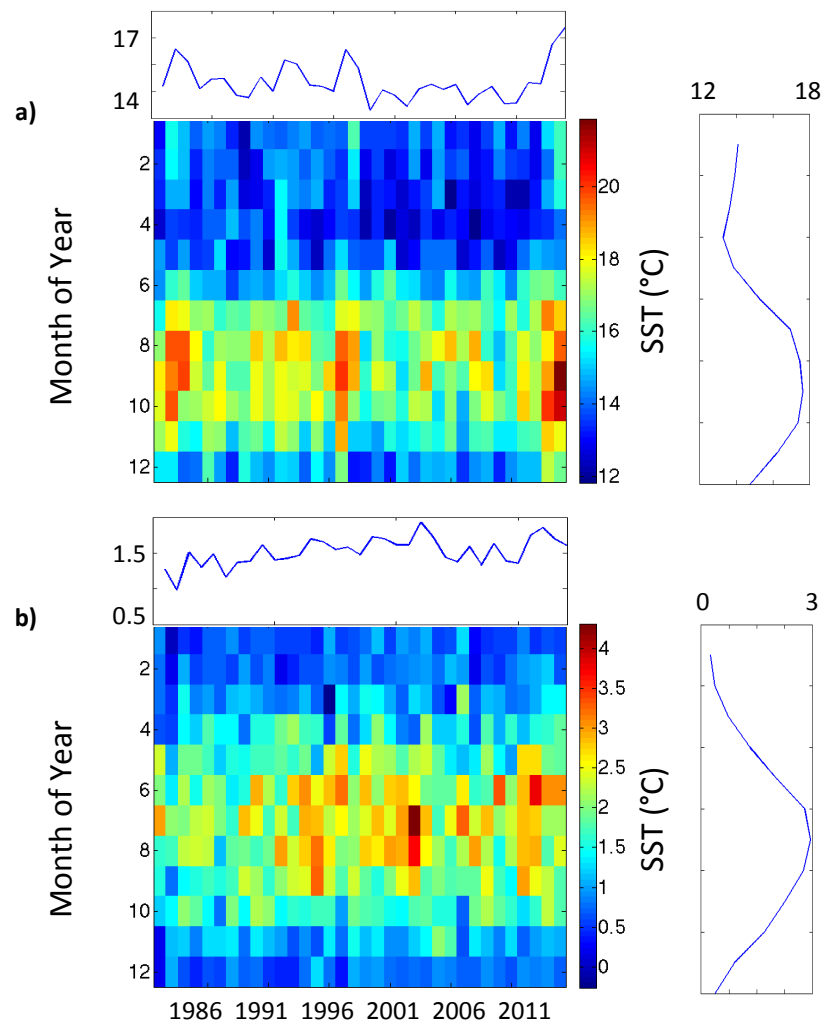
Figure 4.2. Field sampled chlorophyll *a* to carbon ratio (Chl:C) versus canopy Chl:C estimated from hyperspectral Advanced Very High Resolution Radiometer (AVIRIS) imagery.
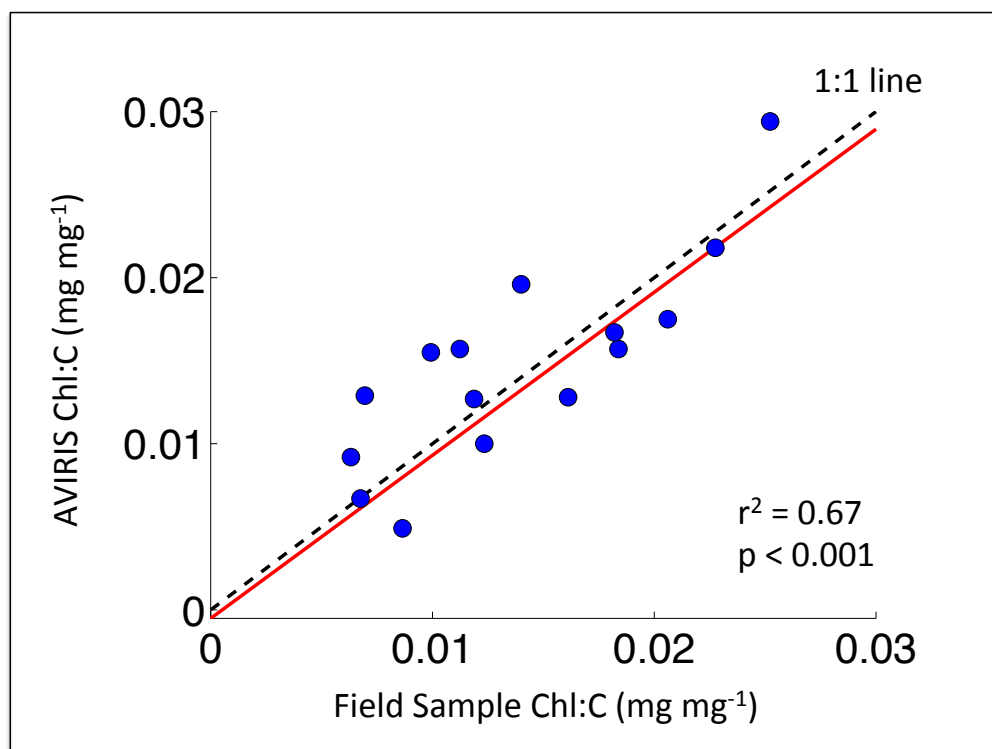
Figure 4.3. Maps showing the mean canopy chlorophyll *a* to carbon ratio (Chl:C) for each 1km coastline segment estimated from hyperspectral Advanced Very High Resolution Radiometer (AVIRIS) imagery. Background of each map showing mean sea surface temperature (SST) for the 8-day period prior to the AVIRIS image date for the Santa Barbara Channel.
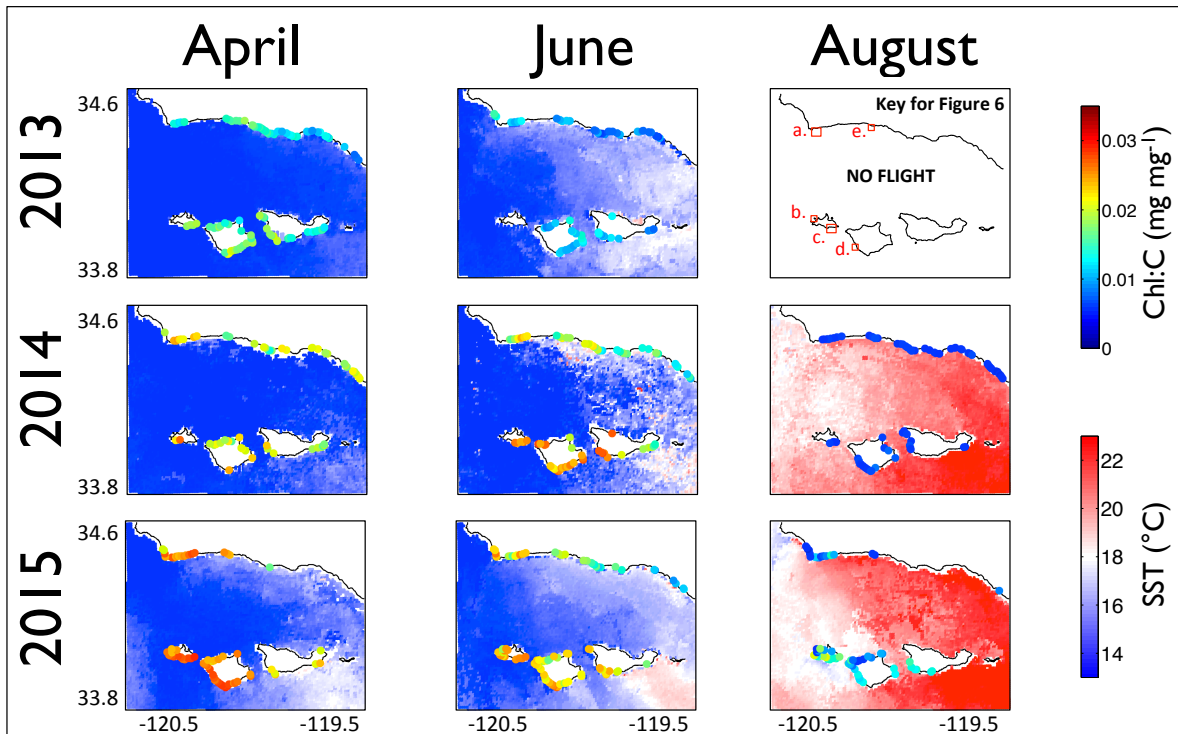
Figure 4.4. Best fit lines between chlorophyll *a* to carbon ratio (Chl:C) for each 1km coastline segment and sea surface temperature (SST) for each image date shown as different colored lines with points. Blue curve represents the mean non-linear relationship for all image dates, shaded area represents 95% confidence interval.
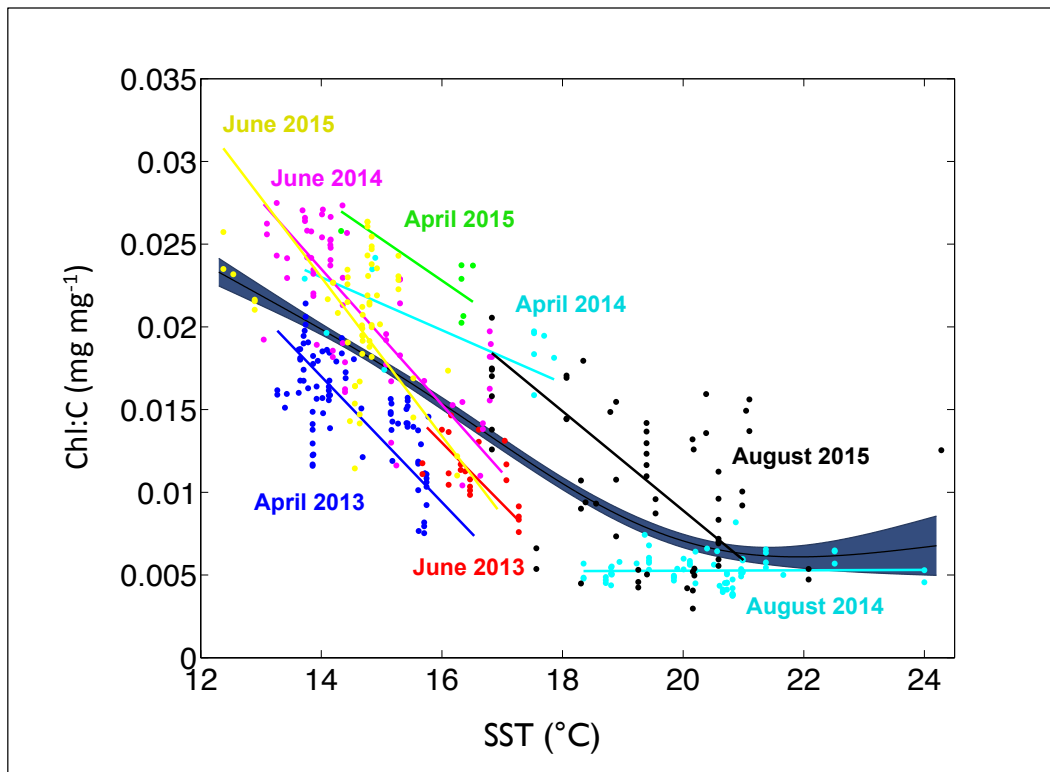
Figure 4.5. Top row shows the canopy chlorophyll *a* to carbon ratio (Chl:C) of the Bulito kelp forest in the western part of the mainland coast of the Santa Barbara Channel at three images dates. The bottom row shows the corresponding kelp canopy fractional cover for each kelp pixel for each date.
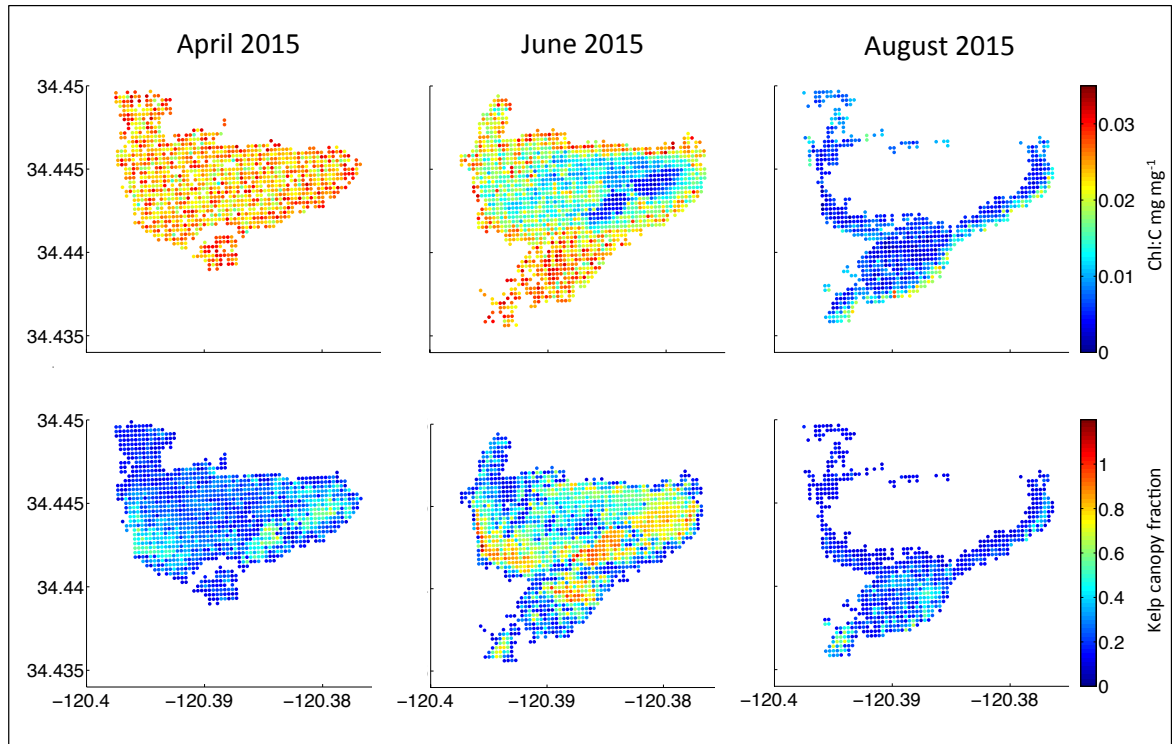
Figure 4.6. Maps of the canopy emergence date (first column) prior to the canopy chlorophyll *a* to carbon ratio (Chl:C) image (second column). The mean Chl:C is shown for each canopy emergence date (error bars show standard error) in the third column. Kelp forests shown are as follows: a) Bulito on the western mainland coast of the Santa Barbara Chanel (SBC) in June 2015, b) western end of San Miguel Island in June 2015, c) southern end of San Miguel Island in August 2015, d) southwestern end of Santa Rosa Island in June 2014, e) Arroyo Quemado kelp forest on the western section of the mainland coast of the SBC in April 2013.
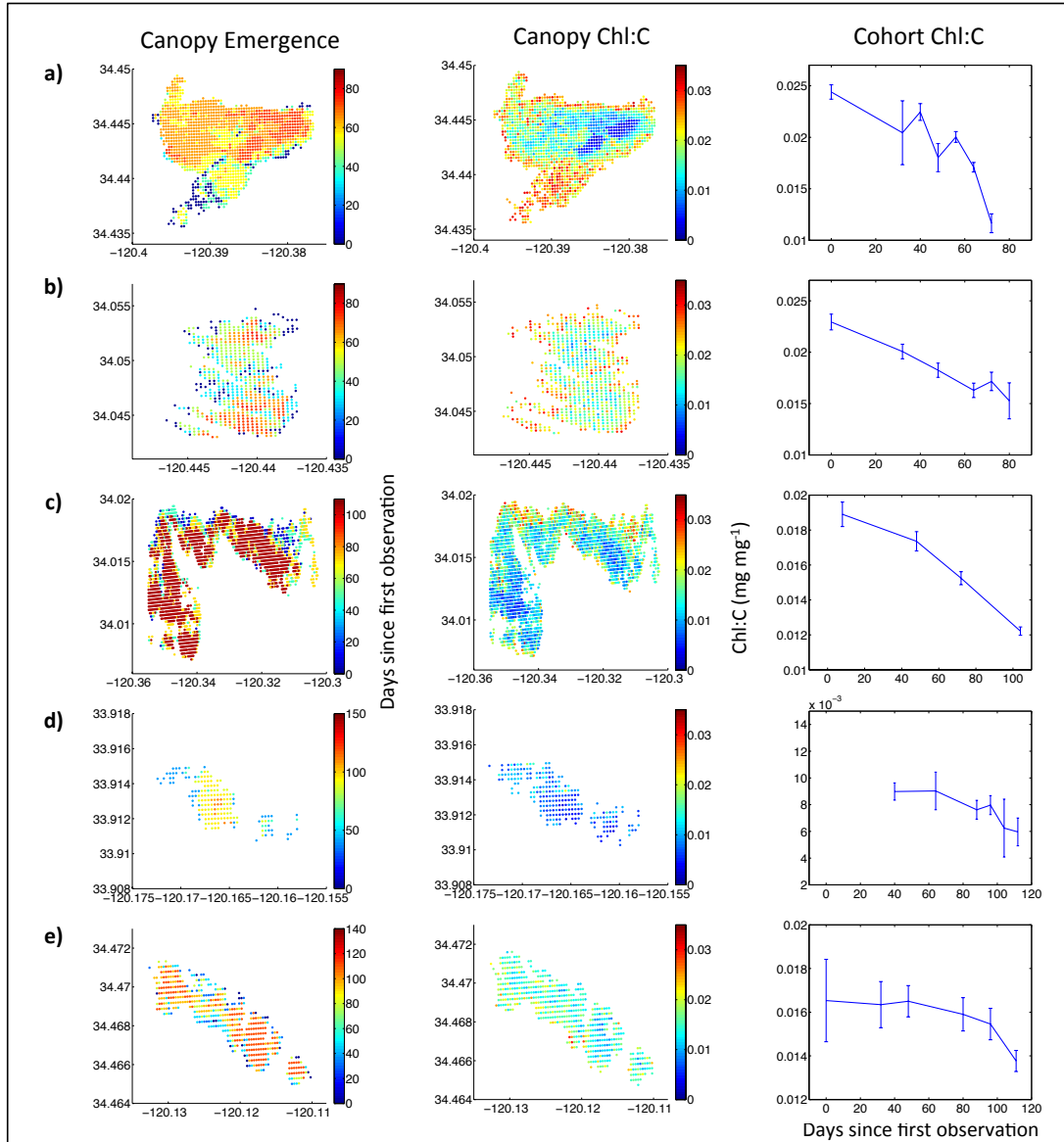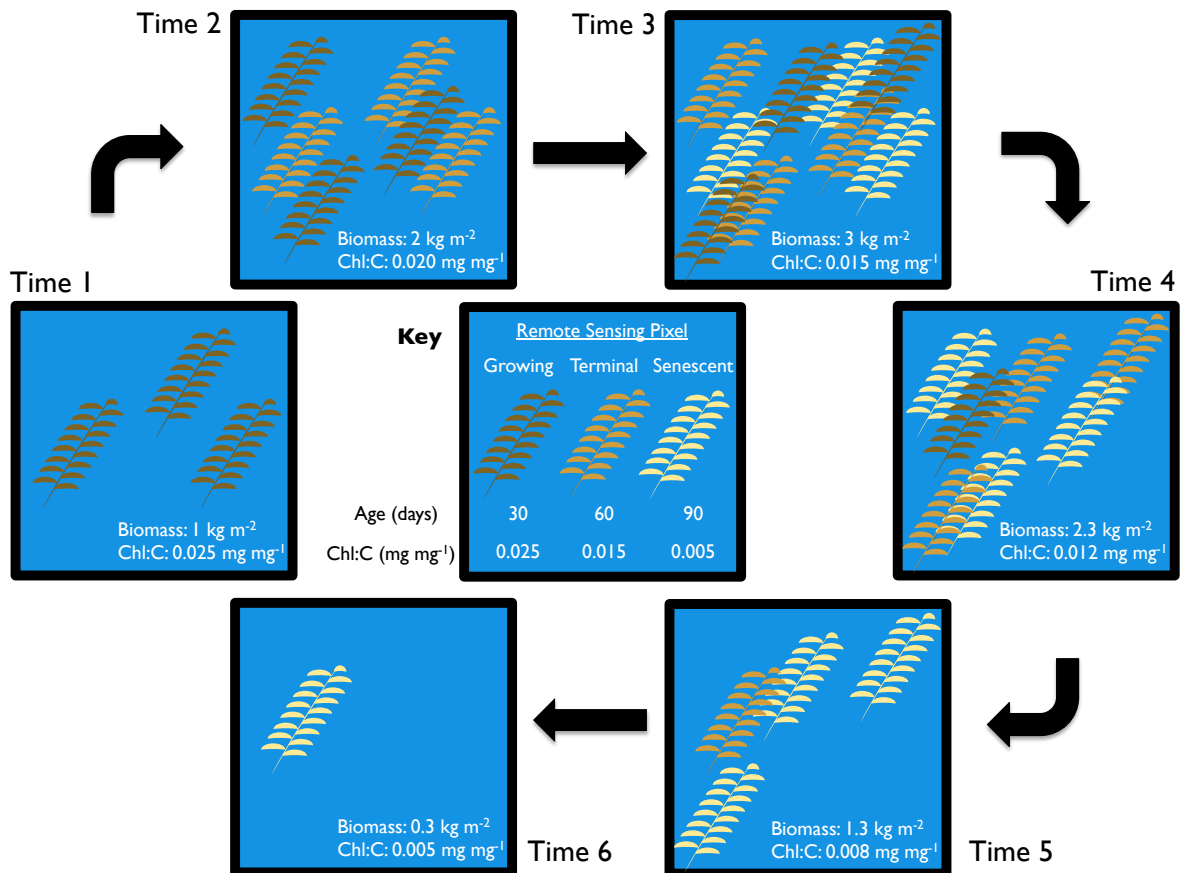
Figure 4.7. Conceptual model of canopy growth and senescence. Each remote sensing pixel represents an average Chl:C of all canopy fronds within it. These fronds can be growing (actively growing apical meristem), terminal (no apical meristem or new blades forming), or senescent. AT time 1 new giant kelp canopy emerges, it will be comprised of all actively growing fronds whose Chl:C is a product of the regional nutrient and light environment. At time 2 these growing fronds age, lose their apical meristem, become a terminal frond, and cease the production of new blades. The blades on these aging fronds will begin to senesce with reductions in photosynthetic performance and Chl:C. Simultaneously new growing fronds emerge and the canopy is mixture of growing and terminal fronds. At time 3 terminal frond become senescent fronds there will be a depression in the mean Chl:C for that pixel as terminal and senescent fronds become a higher proportion of canopy biomass until the addition of new growing fronds equals frond loss through the process of progressive senescence. At time 4 environmental conditions change, and changes in the frond initiation rate, shifting the proportion of new growing fronds in relation to terminal and senescent fronds in the canopy. At time 5, there is a cessation in the initiation of growing fronds only terminal and senescent fronds will form the canopy which will further depress the mean Chl:C. At time 6, only senescent fronds remain and without new frond growth this will lead to eventual canopy loss.

Time 2
Biomass: 2 kg m^{-2}
Chl:C: 0.020 mg mg^{-1}

Time 3
Biomass: 3 kg m^{-2}
Chl:C: 0.015 mg mg^{-1}

Time 1
Biomass: 1 kg m^{-2}
Chl:C: 0.025 mg mg^{-1}

Time 4
Biomass: 2.3 kg m^{-2}
Chl:C: 0.012 mg mg^{-1}

Key

Remote Sensing Pixel

	Growing	Terminal	Senescent
Age (days)	30	60	90
Chl:C (mg mg^{-1})	0.025	0.015	0.005

Time 6
Biomass: 0.3 kg m^{-2}
Chl:C: 0.005 mg mg^{-1}

Time 5
Biomass: 1.3 kg m^{-2}
Chl:C: 0.008 mg mg^{-1}

V. Conclusion

In this dissertation I aimed to answer the overarching question: What are the controls of giant kelp canopy dynamics across space and time? The answer to this question depends on location of the kelp forest in question. Along the central coast of California we observe a regular seasonal cycle with low kelp biomass with a high Chl:C in the winter and high biomass with a low Chl:C in the summer. This pattern suggests a disturbance-modulated system where large swells remove kelp canopy every winter and year round available nutrients allow for robust growth when light levels are adequate. Contrast this with small kelp forests off of the coast of Orange and San Diego counties, which appear for a few years time and then disappear for several years. These forests tend to be associated with the interannual swings of the North Pacific Gyre Oscillation. In fact, the climate scale variations of sea surface temperature, and by extension ambient nitrate concentrations, are explained by this strengthening pattern of the North Pacific Gyre, which advects cool, nutrient-rich water south into the most oligotrophic areas of the Southern California Bight. On top of all of this are demographic patterns associated with frond senescence. The timing of when a kelp forest initiates most of its fronds is going to affect the amount of canopy in the forest when those fronds detach. It is then of utmost importance to incorporate temporal lags into models that will attempt to predict kelp forest dynamics.

The advent of hyperspectral satellite sensors will allow for the determination of giant kelp biomass, emergence time, and Chl:C simultaneously, along with several other characteristics researchers have yet to develop algorithms for. With this wealth of information, we will be much closer to understanding the dynamics of this foundation

species. In the meantime, there are several other avenues of research that will refine our estimates of giant kelp canopy production. First, we can use estimates of available light and seawater nitrate to model canopy Chl:C on subregional scales. We can then use Landsat biomass estimates to model net primary production on a patch scale and hindcast these estimates to at least the 1990's. Production derived from giant kelp can be compared to production from phytoplankton on a subregional scale. These estimates should provide valuable information to ecologists studying how available energy sources are related to community structure and dynamics. Additionally, more work needs to be done relating Chl:C to photosynthetic rates of giant kelp blades. There is evidence that maximum photosynthetic rate decreases with blade age, however this work needs to be extended across time and space. Monthly quantification of the Chl:C and photosynthetic rates of blades from fronds of different ages from the SBC LTER sites would be a great start to this project. These values could easily be used to further refine the giant kelp net primary production model and be incorporated into hyperspectral estimates once they become available.